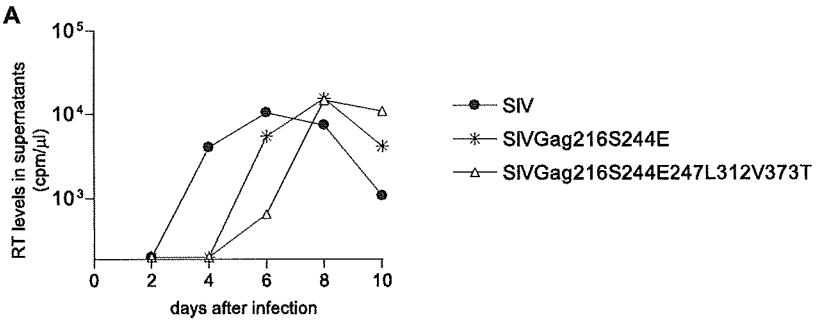

B

Competition between SIVmac239 vs SIVmac239Gag216S244E

inoculated dose ratio 1/1

	day 6	day 18
Exp 1	Wt	Wt
Exp 2	Wt	Wt
Exp 3	Wt (mt)	Wt

Competition between SIVmac239Gag216S244E vs SIVmac239Gag216S244E247L312V373T

	day 6	day 18
Exp 1	Wt	Wt
Exp 2	Wt (mt)	Wt
Exp 3	Wt (mt)	Wt

C

inoculated dose ratio 1/4

	day 6	day 18
SIVmac239	6/13	15/16
SIVmac239Gag216S244E	7/13	1/16

	day 6	day 18
SIVmac239Gag216S244E	7/18	12/16
SIVmac239Gag216S244E247L312V373T	11/18	3/16
*SIVmac239Gag216S244E312V373T		1/16

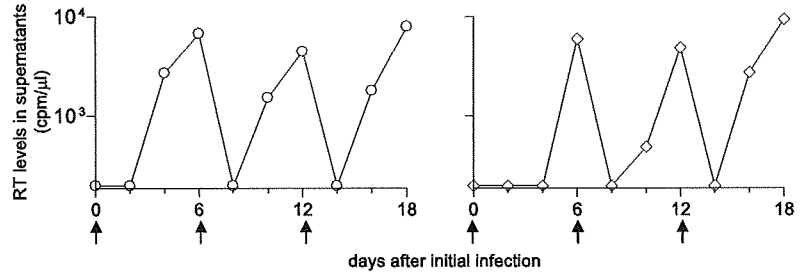

FIG. 1. Replication of mutant SIVs in vitro. (A) Wild-type and mutant SIV replication kinetics in HSC-F cells. HSC-F cells were infected with SIVmac239 (closed circles), SIVmac239Gag216S244E (asterisks), or SIVmac239Gag216S244E247L312V373T (open triangles). Virus production was monitored by measuring RT activity in the culture supernatants. Representative results from three sets of experiments are shown. (B) Viral competition assay. HSC-F cells were coinfected with SIVmac239 and SIVmac239Gag216S244E (left) or with SIVmac239Gag216S244E and SIV mac239Gag216S244E247L312V373T (right) at a ratio of 1:1. Viral *gag* fragments were amplified by RT-PCR from viral RNAs from the culture supernatants at days 6 and 18 postinfection and then sequenced. Dominant amino acid sequences at the 216th and 244th aa (left) or the 247th, 312th, and 373rd aa (right) in Gag in three sets of experiments are shown. Wt, only the wild-type sequence was detected; Wt (mt), the wild type was dominant, but the mutant was detectable (the mutant/wild-type ratio was <1/2). (C) Viral competition assay. HSC-F cells were coinfected with SIVmac239 and SIVmac239Gag216S244E (left) or with SIVmac239Gag216S244E and SIVmac239Gag216S244E247L312V373T (right) at a ratio of 1:4. The amplified *gag* fragments were subcloned into plasmids and sequenced. Frequencies of the indicated SIV clones (number of indicated clone per total number of clones) are shown. Changes in RT levels in the culture supernatants are shown in the bottom panels. The arrows indicate the time points of coinfection (at day 0) and viral passage for the second (at day 6) and the third (at day 12) cultures.

measured by reverse transcription (RT) assay as described previously (25, 33). For analysis of viral replication, HSC-F cells (herpesvirus saimiri-immortalized macaque T-cell line) (1) were infected with wild-type or mutant SIVs (normalized by RT activity), and virus production was monitored by measuring RT activity in the culture supernatants. For competition, HSC-F cells were coinfected with two SIVs at a ratio of 1:1 or 1:4, and the culture supernatants were harvested every other day and used for RT assays. On day 6, the supernatant was added to fresh HSC-F cells to start the second culture. Similarly, on day 12 after the initial coinfection, the second culture supernatant was added to fresh HSC-F cells to start the third culture. RNAs were extracted from the initial culture supernatant on day 6 and from the third culture supernatant on day 18 postcoinfection. The fragment (nucleotides 1231 to 2958 in SIVmac239 [GenBank accession number M33262]) containing the entire *gag* region was amplified from the RNA by RT-PCR and sequenced. Alternatively, it was subcloned into plasmids to determine dominant sequences.

Animal experiments. Burmese rhesus macaques (*Macaca mulatta*) were maintained in accordance with the guidelines for animal experiments performed at the National Institute of Infectious Diseases (26). Three animals, R01-007, R02-003, and R02-012, that received a prophylactic DNA prime/SeV-Gag boost vaccine and contained SIVmac239 challenge have been reported previously (22). In the present study, macaques R06-015, R06-035, R06-041, R05-004, R05-027, and R07-005 also received the DNA prime/SeV-Gag boost vaccine. The DNA used for the vaccination, CMV-SHIVdEN, was constructed from *env*- and *nef*-deleted simian-human immunodeficiency virus $SHIV_{MD14YE}$ molecular clone

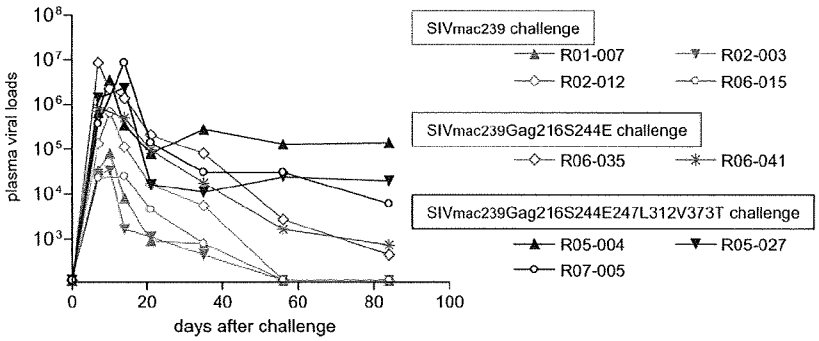

FIG. 2. Plasma viral loads after wild-type or mutant SIV challenge. The *90-120-Ia*-positive vaccinees were challenged with SIVmac239 (red lines), SIVmac239Gag216S244E (blue lines), or SIVmac239Gag216S244E247L312V373T (black lines). Plasma viral loads (SIV *gag* RNA copies/ml plasma) were determined as described before (22). The lower limit of detection is approximately 4×10^2 copies/ml.

DNA (SIVGP1) (31, 32) and has the genes encoding SIVmac239 Gag, Pol, Vif, and Vpx, SIVmac239-HIV chimeric Vpr, and HIV Tat and Rev. At the DNA vaccination, animals received 5 mg of CMV-SHIVdEN DNA intramuscularly. Six weeks after the DNA prime step, animals received a single boost intranasally with 6×10^9 cell infectious units of F-deleted replication-defective SeV-Gag (21, 32). Approximately 3 months after the boost, animals were challenged intravenously with 1,000 50% tissue culture infective doses of SIVmac239, SIVmac239 Gag216S244E, or SIVmac239Gag216S244E247L312V373T. The challenge virus stocks were prepared by virus propagation on rhesus macaque peripheral blood mononuclear cells (PBMCs). Sequence analysis confirmed the absence of *gag* mutations except for the two or five mutations in the challenge viruses.

Immunostaining of $CD4^+$ T-cell memory subsets. PBMCs were subjected to immunofluorescence staining by using fluorescein isothiocyanate-conjugated anti-human CD28, phycoerythrin-conjugated anti-human CD95, peridinin chlorophyll protein-conjugated anti-human CD4, and allophycocyanin-conjugated anti-human CD3 monoclonal antibodies (Becton Dickinson, Tokyo, Japan). The central memory subset of $CD4^+$ T cells was defined by possession of a $CD28^+$ $CD95^+$ phenotype, as described previously (13, 27).

Measurement of virus-specific $CD8^+$ T-cell responses. We measured virus-specific $CD8^+$ T-cell levels by flow cytometric analysis of gamma interferon (IFN-γ) induction after specific stimulation, as described previously (13, 22). In brief, PBMCs were cocultured with autologous herpesvirus papio-immortalized B-lymphoblastoid cell lines infected with a vaccinia virus vector expressing SIVmac239 Gag for Gag-specific stimulation or a vesicular stomatitis virus G protein-pseudotyped SIVGP1 for SIV-specific stimulation. The pseudotyped virus was obtained by cotransfection of COS-1 cells with a vesicular stomatitis virus G protein expression plasmid and the SIVGP1 DNA. Alternatively, B-lymphoblastoid cell lines were pulsed with 1 to 10 μM peptides for peptide-specific stimulation (11, 12). The 15-mer $Gag_{367\text{-}381}$ peptide was used to detect $Gag_{367\text{-}381}$-specific CTLs, including $Gag_{373\text{-}380}$-specific CTLs. Intracellular IFN-γ staining was performed using a Cytofix Cytoperm kit (Becton Dickinson). Peridinin chlorophyll protein-conjugated anti-human CD8, allophycocyanin-conjugated anti-human CD3, and phycoerythrin-conjugated anti-human IFN-γ antibodies (Becton Dickinson) were used. Specific T-cell levels were calculated by subtracting nonspecific IFN-γ^+ T-cell frequencies from those after Gag-specific, SIV-specific, or peptide-specific stimulation. Specific T-cell levels of <100 cells per million PBMCs were considered negative.

Statistical analysis. Statistical analysis was performed with Prism software, version 4.03, with significance set at P values of <0.05 (GraphPad Software, Inc., San Diego, CA). Central memory $CD4^+$ T-cell counts before challenge were not significantly different between the wild-type SIV-challenged ($n = 4$) and the mutant SIV-challenged ($n = 5$) macaques ($P = 0.70$ by unpaired two-tailed t test with Welch's correction and $P = 0.73$ by nonparametric Mann-Whitney U test). Ratios of the central memory $CD4^+$ T-cell counts from a few months postchallenge to those prechallenge were log transformed and compared between the two groups by an unpaired two-tailed t test and the Mann-Whitney U test. Gag-specific $CD8^+$ T-cell frequencies postvaccination (prechallenge) or postchallenge were also log transformed and compared between the two groups in the same statistical manner.

RESULTS

Comparison of viral fitness in wild-type and mutant SIVs. We used two mutant SIVs for challenge of the *90-120-Ia*-positive vaccinees. The first, designated SIVmac239Gag216S244E, carries two *gag* mutations, GagL216S and GagD244E, leading to a leucine (L)-to-serine (S) substitution at the 216th amino acid (aa) and an aspartic acid (D)-to-glutamic acid (E) substitution at the 244th aa in Gag. The second, designated SIVmac239Gag216S244E247L312V373T, carries five *gag* mutations, GagL216S, GagD244E, GagI247L (isoleucine [I] to L at the 247th aa), GagA312V (alanine [A] to valine [V] at the 312th aa), and GagA373T (A to threonine [T] at the 373rd aa). In our previous study (12), the former became dominant in the early phase (at approximately 4 months postchallenge) during the period of viral control, and the latter was dominant at viremia reappearance in a transient controller. GagL216S, GagD244E and GagI247L, and GagA373T mutations result in viral escape from recognition by $Gag_{206\text{-}216}$-specific, $Gag_{241\text{-}249}$-specific, and $Gag_{373\text{-}380}$-specific CTLs, respectively, while it remains unclear whether GagA312V was selected for by CTLs.

We first compared viral fitness in wild-type and mutant SIVs. In HSC-F cells (a macaque T-cell line), not only the wild type but also the mutant SIVs were able to replicate, but SIVmac 239Gag216S244E replication was less efficient than that of wild-type SIVmac239, and SIVmac239Gag216S244E247L312 V373T replication was even less efficient (Fig. 1A). In competitions between two SIVs, HSC-F cells were coinfected with both viruses, and viral genome sequences in the culture supernatants were assessed to establish which SIV became predominant. In culture supernatants of HSC-F cells after coinfection with SIVmac239 and SIVmac239Gag216S244E inoculated at a ratio of 1:1, the wild type rapidly became dominant (at day 6) (Fig. 1B). Coinfection at a ratio of 1:4 resulted in equivalence at day 6, but the wild type again dominated by day 18 (Fig. 1C). These results indicate a lower replicative ability of SIVmac239 Gag216S244E than of wild-type SIVmac239. In addition, competition between SIVmac239Gag216S244E and SIVmac239 Gag216S244E247L312V373T showed the lower replicative ability of the latter (Fig. 1B and C).

Challenge of *90-120-Ia*-positive vaccinees with wild-type or mutant SIVs. Next, we challenged *90-120-Ia*-positive macaques

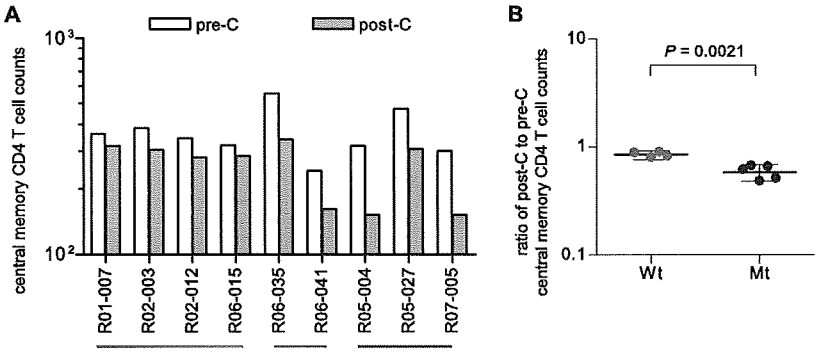

FIG. 3. Changes in central memory $CD4^+$ T-cell counts after wild-type or mutant SIV challenge. (A) Peripheral central memory $CD4^+$ ($CD4^+$ $CD95^+$ $CD28^+$) T-cell counts (/μl) prechallenge (pre-C) and a few months postchallenge (post-C). (B) Statistical comparison of central memory $CD4^+$ T-cell loss between the wild-type SIV-challenged (Wt) and the mutant SIV-challenged (Mt) macaques. The ratios of central memory $CD4^+$ T-cell counts postchallenge to those prechallenge are plotted. The longer bars indicate geometric mean values, and the regions between the shorter bars indicate the 95% confidence intervals. The ratios in the mutant group (n = 5) were significantly lower than those in the wild-type group (n = 4) (P = 0.0021 by unpaired t test and P = 0.0159 by Mann-Whitney U test).

with the mutant SIVs after DNA prime/SeV-Gag vaccination. Remarkably, all three vaccinees (R05-004, R05-027, and R07-005) challenged with SIVmac239Gag216S244E247L312V373T failed to control viral replication and showed high set point plasma viral loads, while all four vaccinees (R01-007, R02-003, R02-012, and R06-015) challenged with wild-type SIVmac239 contained viral replication, with undetectable set point plasma viral loads (Fig. 2). Even the two vaccinees (R06-035 and R06-041) challenged with SIVmac239Gag216S244E failed to contain viral replication, although with lower plasma viral loads, at approximately 10^3 RNA copies/ml at 3 months postchallenge. Central memory $CD4^+$ T-cell counts before challenge were not significantly different between the wild-type SIV-challenged (n = 4) and mutant SIV-challenged (n = 5) macaques, but ratios of the counts at a few months postchallenge to prechallenge for the latter group were significantly lower than those for the former (P = 0.0021 by unpaired t test and P = 0.0159 by Mann-Whitney U test) (Fig. 3). Thus, *90-120-Ia*-positive vaccinees can contain wild-type SIVmac239 but not SIVmac239Gag216S244E or SIVmac239Gag216S244E247L312V373T challenge.

Viral *gag* sequence analysis confirmed the rapid selection for the GagL216S mutation in all wild-type SIVmac239-challenged macaques, as described previously (22). All of the *gag* mutations in the challenge mutant viruses were maintained during the observation period (Table 1). SIVmac239Gag216S244E247L312V373T-challenged macaques showed no additional dominant *gag* mutations, whereas animals challenged with SIVmac239Gag216S244E rapidly selected viruses with a GagV145A (V to A at the 145th aa) mutation. Recovery of viral fitness by this mutation was not observed, and whether it was selected for by CTLs was unclear in our previous study (12).

Gag-specific CTL responses were induced after SeV-Gag boost in all vaccinees, and there was no significant difference in the levels between the wild-type and mutant challenges (P = 0.1198 by unpaired t test and P = 0.1111 by Mann-Whitney U test). However, secondary Gag-specific CTL responses were

TABLE 1. Dominant sequences in SIV Gag in macaques after challenge

Macaque	Time (wk) of plasma sample	Amino acid change in Gag at position[a]:								
		140	145	206	216	244	247	312	341	373
R01-007	5				L216S					
R02-003	5				L216S					
R02-012	5				L216S					
R06-015	5			(I206M)	L216S					
R06-035	5				L216S*	D244E*				
	12		V145A		L216S*	D244E*			(N341Y)	
R06-041	5		(V145A)		L216S*	D244E*				
	12		V145A		L216S*	D244E*				
R05-004	5				L216S*	D244E*	I247L*	A312V*		A373T*
	12	(I140V)			L216S*	D244E*	I247L*	A312V*		A373T*
R05-027	5				L216S*	D244E*	I247L*	A312V*		A373T*
	12				L216S*	D244E*	I247L*	A312V*		A373T*
R07-005	5				L216S*	D244E*	I247L*	A312V*		A373T*
	12				L216S*	D244E*	I247L*	A312V*		A373T*

[a] A fragment containing the entire *gag* region was amplified from plasma RNA by nested RT-PCR and then sequenced. We were unable to amplify the fragment from plasmas obtained at week 12 from the wild-type SIVmac239-challenged macaques with undetectable viremia. Dominant *gag* mutations resulting in amino acid changes are shown. Asterisks indicate the mutations included in the challenge inoculums. Parentheses indicate that both the wild-type and mutant sequences were detected equivalently at that position.

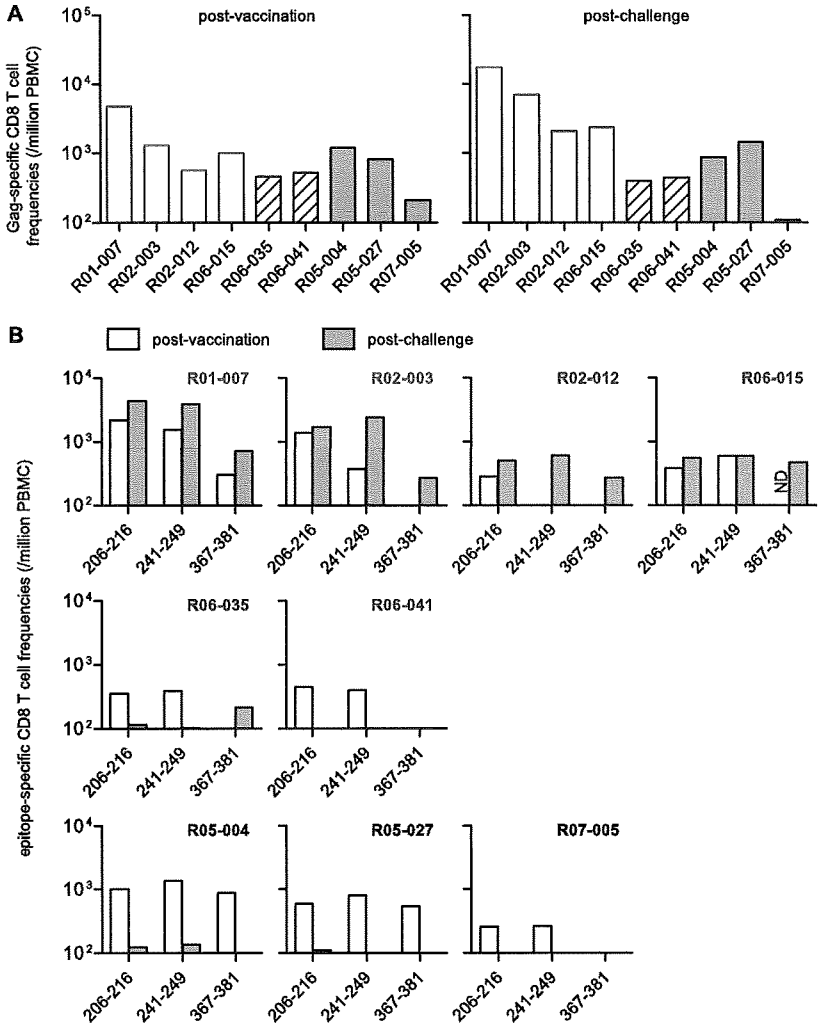

FIG. 4. Gag-specific $CD8^+$ T-cell responses before and after wild-type or mutant SIV challenge. Macaques R01-007, R02-003, R02-012, and R06-015 were challenged with SIVmac239; macaques R06-035 and R06-041 were challenged with SIVmac239Gag216S244E; and macaques R05-004, R05-027, and R07-005 were challenged with SIVmac239Gag216S244E247L312V373T. (A) Gag-specific $CD8^+$ T-cell frequencies at 2 weeks postboost (postvaccination) (left) and 2 weeks postchallenge (right). (B) $Gag_{206-216}$-specific, $Gag_{241-249}$-specific, and $Gag_{367-381}$-specific $CD8^+$ T-cell frequencies at 2 weeks (all except for R02-012) or 4 weeks (in R02-012) postboost (postvaccination) and 5 weeks (in R01-007, R02-003, R02-012, R06-035, R06-041, and R05-004) or 6 weeks (in R06-015, R05-027, and R07-005) postchallenge. ND, not determined.

less efficient after challenge with mutant SIV than after challenge with wild-type SIV ($P = 0.0095$ by unpaired t test and $P = 0.0159$ by Mann-Whitney U test) (Fig. 4A).

SeV-Gag boost induced efficient $Gag_{206-216}$-specific and $Gag_{241-249}$-specific CTL responses in all vaccinees and $Gag_{367-381}$-specific CTL responses in some of them (Fig. 4B). Challenge with wild-type SIVmac239 resulted in efficient secondary responses of these three epitope-specific CTLs, whereas SIVmac 239Gag216S244E247L312V373T challenge evoked none of them (Fig. 4B). SIVmac239Gag216S244E challenge did not result in secondary responses of $Gag_{206-216}$-specific or $Gag_{241-249}$-specific CTLs but did induce $Gag_{367-381}$-specific CTL responses in one case (Fig. 4B). These results indicate that SIVmac239 Gag216S244E evades recognition by $Gag_{206-216}$-specific and $Gag_{241-249}$-specific CTLs and that SIVmac239Gag216S244E2 47L312V373T evades recognition by $Gag_{206-216}$-specific, $Gag_{241-249}$-specific, and $Gag_{367-381}$-specific CTLs.

We next examined Gag-specific and SIV-specific CTL responses after mutant SIV challenge (Fig. 5A). We used an *env*- and *nef*-deleted SHIV molecular clone DNA, SIVGP1, that has the genes encoding SIVmac239 Gag, Pol, Vif, Vpx, and a part of Vpr and measured the frequencies of CTLs responding to SIVGP1-transduced cells (referred to as SIV-specific CTLs) as described previously (13, 32). SIV-specific CTL frequencies at week 12 were much higher than those at week 2 for all five macaques challenged with mutant SIVs. In contrast, Gag-specific CTL frequencies at week 12 were lower than those at week 2 for four of five animals; the remaining macaque, R06-035, mounted $Gag_{367-381}$-specific CTL responses. Importantly, in all animals challenged with mutant SIVs, SIV-specific CTL

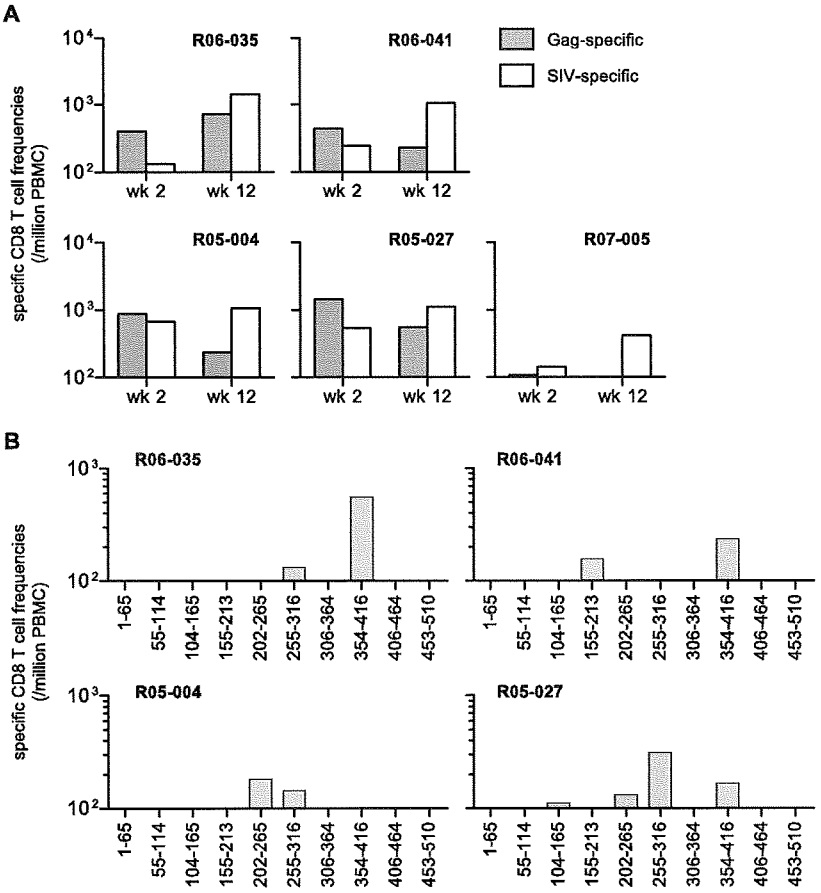

FIG. 5. SIV-specific $CD8^+$ T-cell responses after mutant SIV challenge. (A) Gag-specific (closed boxes) and SIV-specific (open boxes) $CD8^+$ T-cell frequencies at 2 weeks or 12 weeks postchallenge. (B) Frequencies of $CD8^+$ T cells specific for pools of SIV Gag peptides. A panel of 117 overlapping peptides (15 to 17 aa in length and overlapping by 10 to 12 aa) spanning the entire SIV Gag amino acid sequence were divided into the following 10 pools (each consisting of 11 or 12 peptides): pool 1, 1st to 65th aa in SIV Gag; pool 2, 55th to 114th aa; pool 3, 104th to 165th aa; pool 4, 155th to 213th aa; pool 5, 202nd to 265th aa; pool 6, 255th to 316th aa; pool 7, 306th to 364th aa; pool 8, 354th to 416th aa; pool 9, 406th to 464th aa; and pool 10, 453rd to 510th aa. The pools were used for stimulation to detect peptide pool-specific $CD8^+$ T cells.

frequencies were at marginal levels or lower than Gag-specific CTL frequencies at week 2, but the former became higher than the latter at week 12. These results indicate an induction of CTL responses specific for SIV antigens other than Gag in all five macaques after mutant SIV challenge.

At week 12 after mutant SIV challenge, Gag-specific CTL responses were undetectable in macaque R07-005 but were still detected in the other four macaques. We then analyzed Gag-specific CTL responses in these four macaques by using a panel of overlapping peptides spanning the entire SIV Gag amino acid sequence (Fig. 5B). In both SIVmac239Gag216S2 44E-challenged animals, R06-035 and R06-041, exhibiting detectable $Gag_{367-381}$-specific CTL responses (data not shown), CTL responses specific for the peptide mixture corresponding to the 354th to 416th aa in SIV Gag were detected at week 12. In addition, we found $Gag_{255-316}$-specific CTL responses in macaque R06-035 and $Gag_{155-213}$-specific CTL responses in macaque R06-041. SIVmac239Gag216S244E247L312V373T-challenged macaques R05-004 and R05-027 showed responses specific for several Gag peptide mixtures, including $Gag_{202-265}$-specific and $Gag_{255-316}$-specific CTL responses. These results indicate an induction of CTL responses specific for Gag epitopes other than the $Gag_{206-216}$, $Gag_{241-249}$, and $Gag_{373-380}$ epitopes after mutant SIV challenge.

DISCUSSION

In the present study, SIVs carrying multiple *gag* CTL escape mutations showed lower replicative abilities than that of the wild type; nonetheless, the *90-120-Ia*-positive vaccinees were able to contain only the latter. This demonstrates that Gag-specific CTL responses did play a central role in the vaccine-based primary containment of wild-type SIVmac239 replication in *90-120-Ia*-positive macaques.

Elicitation of virus-specific T-cell responses by prophylactic vaccination is believed to be a promising strategy for HIV control (3, 24); whether this approach can actually result in HIV control remains unknown. Recent studies have indicated the possibility of reductions in set point viral loads after SIV challenge by prophylactic vaccination inducing T-cell responses in rhesus macaques (19, 22, 34), yet the immune component crucial for the vaccine-based viral control has not been

determined. No clear evidence for a contribution of vaccine-induced CTLs to this viral control has been forthcoming to date, although virus-specific CTL responses have been implicated in exerting strong suppressive pressure on HIV/SIV infection (9, 22). Indeed, viral replication persists even in the presence of CTL responses in the natural course of infection; it has thus remained unclear whether HIV/SIV replication can be controlled by vaccine-induced CTLs. The evidence from the present study now strongly implicates Gag-specific CTL responses as responsible for vaccine-based primary SIV control. This offers the possibility of Gag-specific CTL-based HIV containment by prophylactic vaccination and provides insight into the development of CTL-based AIDS vaccines.

The containment of SIVmac239 but failure to contain SIV mac239Gag216S244E in the vaccinees documents a crucial role for $Gag_{206-216}$-specific and/or $Gag_{241-249}$-specific CTL responses in vaccine-based SIVmac239 containment. Furthermore, challenge with SIVmac239Gag216S244E247L312V373T, possessing diminished viral fitness compared to SIVmac239Gag216S244E, tended to result in higher viral loads, indicating the involvement of $Gag_{373-380}$-specific CTL responses in viral control, while more complete viral evasion of $Gag_{241-249}$-specific CTL recognition by addition of the GagI247L mutation may also contribute to the difference between SIVmac239Gag216S244E and SIVmac239Gag216S244E247L312V373T challenge. Taken together, we conclude that these two or three epitope-specific CTL responses are crucial for primary SIVmac239 control in *90-120-Ia*-positive vaccinees. Conversely, this study implies that viral evasion of recognition by two dominant epitope-specific CTLs can result in failure of primary viral containment but may not be sufficient for abrogation of vaccine efficacy. Thus, analysis of CTL-based vaccine efficacy against SIVs carrying single or multiple CTL escape mutations could contribute to an evaluation of its potential for controlling the replication of highly diversified HIVs.

Our results suggest that SIV- but non-Gag-specific CTLs became predominant after mutant SIV challenge. Additionally, CTLs recognizing Gag regions other than the $Gag_{206-216}$, $Gag_{241-249}$, and $Gag_{373-380}$ epitopes were detected in most cases. These CTL responses may exert suppressive pressure on viral replication but are considered insufficient for controlling replication of the mutant SIVs with lower viral fitness.

Finally, this study also provides evidence indicating a possible abrogation of CTL-based AIDS vaccine efficacy in viral transmission between MHC-I-matched individuals. Indeed, even the mutant SIVs carrying multiple CTL escape mutations were able to replicate persistently in vivo, despite their diminished replicative ability. Transmission of these viruses can result in persistent viral infection and AIDS progression (30). CTL escape mutations resulting in a loss of viral fitness may revert to the wild-type sequence after transmission into MHC-I-mismatched hosts (4, 8, 9, 16, 18, 20), but such reversion does not occur rapidly; alternatively, some may be retained with additional compensatory mutations (6, 7, 30). Thus, there may be a risk of transmission and accumulation of HIV CTL escape variants even among MHC-I-mismatched individuals, resulting in abrogation of CTL-based AIDS vaccine efficacy in a population.

ACKNOWLEDGMENTS

This work was supported by grants from the Ministry of Education, Culture, Sports, Science, and Technology, by a grant from the Japan Health Sciences Foundation, and by grants from the Ministry of Health, Labor, and Welfare in Japan.

The animal experiments were conducted through the Cooperative Research Program in Tsukuba Primate Research Center, National Institute of Biomedical Innovation, with the help of the Corporation for Production and Research of Laboratory Primates. We thank DNAVEC Corp., H. Igarashi, F. Ono, A. Hiyaoka, K. Oto, Y. Yasutomi, M. Miyazawa, A. Kimura, K. Mori, N. Yamamoto, T. Kurata, Y. Nagai, and A. Nomoto for their help.

REFERENCES

1. **Akari, H., K. Mori, K. Terao, I. Otani, M. Fukasawa, R. Mukai, and Y. Yoshikawa.** 1996. In vitro immortalization of Old World monkey T lymphocytes with herpesvirus saimiri: its susceptibility to infection with simian immunodeficiency viruses. Virology **218**:382–388.
2. **Borrow, P., H. Lewicki, B. H. Hahn, G. M. Shaw, and M. B. Oldstone.** 1994. Virus-specific $CD8^+$ cytotoxic T-lymphocyte activity associated with control of viremia in primary human immunodeficiency virus type 1 infection. J. Virol. **68**:6103–6110.
3. **Brander, C., and B. D. Walker.** 1999. T lymphocyte responses in HIV-1 infection: implication for vaccine development. Curr. Opin. Immunol. **11**: 451–459.
4. **Brander, C., and B. D. Walker.** 2003. Gradual adaptation of HIV to human host populations: good or bad news? Nat. Med. **9**:1359–1362.
5. **Cohen, J.** 2007. Did Merck's failed HIV vaccine cause harm? Science **318**: 1048–1049.
6. **Crawford, H., J. G. Prado, A. Leslie, S. Hué, I. Honeyborne, S. Reddy, M. van der Stok, Z. Mncube, C. Brander, C. Rousseau, J. I. Mullins, R. Kaslow, P. Goepfert, S. Allen, E. Hunter, J. Mulenga, P. Kiepiela, B. D. Walker, and P. J. R. Goulder.** 2007. Compensatory mutation partially restores fitness and delays reversion of escape mutation within the immunodominant HLA-B*5703-restricted Gag epitope in chronic human immunodeficiency virus type 1 infection. J. Virol. **81**:8346–8351.
7. **Friedrich, T. C., C. A. Frye, L. J. Yant, D. H. O'Connor, N. A. Kriewaldt, M. Benson, L. Vojnov, E. J. Dodds, C. Cullen, R. Rudersdorf, A. L. Hughes, N. Wilson, and D. I. Watkins.** 2004. Extra-epitopic compensatory substitutions partially restore fitness to simian immunodeficiency virus variants that escape from an immunodominant cytotoxic T-lymphocyte response. J. Virol. **78**:2581–2585.
8. **Friedrich, T. C., E. J. Dodds, L. J. Yant, L. Vojnov, R. Rudersdorf, C. Cullen, D. T. Evans, R. C. Desrosiers, B. R. Mothe, J. Sidney, A. Sette, K. Kunstman, S. Wolinsky, M. Piatak, J. Lifson, A. L. Hughes, N. Wilson, D. H. O'Connor, and D. I. Watkins.** 2004. Reversion of CTL escape-variant immunodeficiency viruses in vivo. Nat. Med. **10**:275–281.
9. **Goulder, P. J., and D. I. Watkins.** 2004. HIV and SIV CTL escape: implications for vaccine design. Nat. Rev. Immunol. **4**:630–640.
10. **Jin, X., D. E. Bauer, S. E. Tuttleton, S. Lewin, A. Gettie, J. Blanchard, C. E. Irwin, J. T. Safrit, J. Mittler, L. Weinberger, L. G. Kostrikis, L. Zhang, A. S. Perelson, and D. D. Ho.** 1999. Dramatic rise in plasma viremia after CD8+ T cell depletion in simian immunodeficiency virus-infected macaques. J. Exp. Med. **189**:991–998.
11. **Kato, M., H. Igarashi, A. Takeda, Y. Sasaki, H. Nakamura, M. Kano, T. Sata, A. Iida, M. Hasegawa, S. Horie, E. Higashihara, Y. Nagai, and T. Matano.** 2005. Induction of Gag-specific T-cell responses by therapeutic immunization with a Gag-expressing Sendai virus vector in macaques chronically infected with simian-human immunodeficiency virus. Vaccine **23**:3166–3173.
12. **Kawada, M., H. Igarashi, A. Takeda, T. Tsukamoto, H. Yamamoto, S. Dohki, M. Takiguchi, and T. Matano.** 2006. Involvement of multiple epitope-specific cytotoxic T-lymphocyte responses in vaccine-based control of simian immunodeficiency virus replication in rhesus macaques. J. Virol. **80**:1949–1958.
13. **Kawada, M., T. Tsukamoto, H. Yamamoto, A. Takeda, H. Igarashi, D. I. Watkins, and T. Matano.** 2007. Long-term control of simian immunodeficiency virus replication with central memory $CD4^+$ T-cell preservation after nonsterile protection by a cytotoxic T-lymphocyte-based vaccine. J. Virol. **81**:5202–5211.
14. **Kestler, H. W., III, D. J. Ringler, K. Mori, D. L. Panicali, P. K. Sehgal, M. D. Daniel, and R. C. Desrosiers.** 1991. Importance of the nef gene for maintenance of high virus loads and for development of AIDS. Cell **65**:651–662.
15. **Kiepiela, P., K. Ngumbela, C. Thobakgale, D. Ramduth, I. Honeyborne, E. Moodley, S. Reddy, C. de Pierres, Z. Mncube, N. Mkhwanazi, K. Bishop, M. van der Stok, K. Nair, N. Khan, H. Crawford, R. Payne, A. Leslie, J. Prado, A. Prendergast, J. Frater, N. McCarthy, C. Brander, G. H. Learn, D. Nickle, C. Rousseau, H. Coovadia, J. I. Mullins, D. Heckerman, B. D. Walker, and P. Goulder.** 2007. CD8+ T-cell responses to different HIV proteins have discordant associations with viral load. Nat. Med. **13**:46–53.

16. **Kobayashi, M., H. Igarashi, A. Takeda, M. Kato, and T. Matano.** 2005. Reversion in vivo after inoculation of a molecular proviral DNA clone of simian immunodeficiency virus with a cytotoxic-T-lymphocyte escape mutation. J. Virol. **79:**11529–11532.
17. **Koup, R. A., J. T. Safrit, Y. Cao, C. A. Andrews, G. McLeod, W. Borkowsky, C. Farthing, and D. D. Ho.** 1994. Temporal association of cellular immune responses with the initial control of viremia in primary human immunodeficiency virus type 1 syndrome. J. Virol. **68:**4650–4655.
18. **Leslie, A. J., K. J. Pfafferott, P. Chetty, R. Draenert, M. M. Addo, M. Feeney, Y. Tang, E. C. Holmes, T. Allen, J. G. Prado, M. Altfeld, C. Brander, C. Dixon, D. Ramduth, P. Jeena, S. A. Thomas, A. St. John, T. A. Roach, B. Kupfer, G. Luzzi, A. Edwards, G. Taylor, H. Lyall, G. Tudor-Williams, V. Novelli, J. Martinez-Picado, P. Kiepiela, B. D. Walker, and P. J. Goulder.** 2004. HIV evolution: CTL escape mutation and reversion after transmission. Nat. Med. **10:**282–289.
19. **Letvin, N. L., J. R. Mascola, Y. Sun, D. A. Gorgone, A. P. Buzby, L. Xu, Z. Y. Yang, B. Chakrabarti, S. S. Rao, J. E. Schmitz, D. C. Montefiori, B. R. Barker, F. L. Bookstein, and G. J. Nabel.** 2006. Preserved CD4+ central memory T cells and survival in vaccinated SIV-challenged monkeys. Science **312:**1530–1533.
20. **Li, B., A. D. Gladden, M. Altfeld, J. M. Kaldor, D. A. Cooper, A. D. Kelleher, and T. M. Allen.** 2007. Rapid reversion of sequence polymorphisms dominates early human immunodeficiency virus type 1 evolution. J. Virol. **81:**193–201.
21. **Li, H. O., Y. F. Zhu, M. Asakawa, H. Kuma, T. Hirata, Y. Ueda, Y. S. Lee, M. Fukumura, A. Iida, A. Kato, Y. Nagai, and M. Hasegawa.** 2000. A cytoplasmic RNA vector derived from nontransmissible Sendai virus with efficient gene transfer and expression. J. Virol. **74:**6564–6569.
22. **Matano, T., M. Kobayashi, H. Igarashi, A. Takeda, H. Nakamura, M. Kano, C. Sugimoto, K. Mori, A. Iida, T. Hirata, M. Hasegawa, T. Yuasa, M. Miyazawa, Y. Takahashi, M. Yasunami, A. Kimura, D. H. O'Connor, D. I. Watkins, and Y. Nagai.** 2004. Cytotoxic T lymphocyte-based control of simian immunodeficiency virus replication in a preclinical AIDS vaccine trial. J. Exp. Med. **199:**1709–1718.
23. **Matano, T., R. Shibata, C. Siemon, M. Connors, H. C. Lane, and M. A. Martin.** 1998. Administration of an anti-CD8 monoclonal antibody interferes with the clearance of chimeric simian/human immunodeficiency virus during primary infections of rhesus macaques. J. Virol. **72:**164–169.
24. **McMichael, A. J., and T. Hanke.** 2003. HIV vaccines 1983–2003. Nat. Med. **9:**874–880.
25. **Miyagi, E., S. Opi, H. Takeuchi, M. Khan, R. Goila-Gaur, S. Kao, and K. Strebel.** 2007. Enzymatically active APOBEC3G is required for efficient inhibition of human immunodeficiency virus type 1. J. Virol. **81:**13346–13353.
26. **National Institute of Infectious Diseases.** 2007. Guides for animal experiments performed at National Institute of Infectious Diseases. National Institute of Infectious Diseases, Tokyo, Japan. (In Japanese.)
27. **Pitcher, C. J., S. I. Hagen, J. M. Walker, R. Lum, B. L. Mitchell, V. C. Maino, M. K. Axthelm, and L. J. Picker.** 2004. Development and homeostasis of T cell memory in rhesus macaques. J. Immunol. **168:**29–43.
28. **Sacha, J. B., C. Chung, E. G. Rakasz, S. P. Spencer, A. K. Jonas, A. T. Bean, W. Lee, B. J. Burwitz, J. J. Stephany, J. T. Loffredo, D. B. Allison, S. Adnan, A. Hoji, N. A. Wilson, T. C. Friedrich, J. D. Lifson, O. O. Yang, and D. I. Watkins.** 2007. Gag-specific CD8+ T lymphocytes recognize infected cells before AIDS-virus integration and viral protein expression. J. Immunol. **178:**2746–2754.
29. **Schmitz, J. E., M. J. Kuroda, S. Santra, V. G. Sasseville, M. A. Simon, M. A. Lifton, P. Racz, K. Tenner-Racz, M. Dalesandro, B. J. Scallon, J. Ghrayeb, M. A. Forman, D. C. Montefiori, E. P. Rieber, N. L. Letvin, and K. A. Reimann.** 1999. Control of viremia in simian immunodeficiency virus infection by CD8+ lymphocytes. Science **283:**857–860.
30. **Seki, S., M. Kawada, A. Takeda, H. Igarashi, T. Sata, and T. Matano.** 2008. Transmission of simian immunodeficiency virus carrying multiple cytotoxic-T-lymphocyte escape mutations with diminished replicative ability can result in AIDS progression in rhesus macaques. J. Virol. **82:**5093–5098.
31. **Shibata, R., F. Maldarelli, C. Siemon, T. Matano, M. Parta, G. Miller, T. Fredrickson, and M. A. Martin.** 1997. Infection and pathogenicity of chimeric simian-human immunodeficiency viruses in macaques: determinants of high virus loads and CD4 cell killing. J. Infect. Dis. **176:**362–373.
32. **Takeda, A., H. Igarashi, H. Nakamura, M. Kano, A. Iida, T. Hirata, M. Hasegawa, Y. Nagai, and T. Matano.** 2003. Protective efficacy of an AIDS vaccine, a single DNA-prime followed by a single booster with a recombinant replication-defective Sendai virus vector, in a macaque AIDS model. J. Virol. **77:**9710–9715.
33. **Willey, R. L., D. H. Smith, L. A. Lasky, T. S. Theodore, P. L. Earl, B. Moss, D. J. Capon, and M. A. Martin.** 1988. In vitro mutagenesis identifies a region within the envelope gene of the human immunodeficiency virus that is critical for infectivity. J. Virol. **62:**139–147.
34. **Wilson, N. A., J. Reed, G. S. Napoe, S. Piaskowski, A. Szymanski, J. Furlott, E. J. Gonzalez, L. J. Yant, N. J. Maness, G. E. May, T. Soma, M. R. Reynolds, E. Rakasz, R. Rudersdorf, A. B. McDermott, D. H. O'Connor, T. C. Friedrich, D. B. Allison, A. Patki, L. J. Picker, D. R. Burton, J. Lin, L. Huang, D. Patel, G. Heindecker, J. Fan, M. Citron, M. Horton, F. Wang, X. Liang, J. W. Shiver, D. R. Casimiro, and D. I. Watkins.** 2006. Vaccine-induced cellular immune responses reduce plasma viral concentrations after repeated low-dose challenge with pathogenic simian immunodeficiency virus SIVmac239. J. Virol. **80:**5875–5885.

ELSEVIER

INSTITUT PASTEUR

Microbes and Infection 10 (2008) 396–404

www.elsevier.com/locate/micinf

Original article

A rapid recombination assay of HIV-1 using murine CD52 as a novel biomarker

Jun-ichi Sakuragi*, Sayuri Sakuragi, Masahisa Ohishi, Tatsuo Shioda

Department of Viral Infections, Research Institute for Microbial Diseases, Osaka University, Osaka, Japan

Received 11 October 2007; accepted 30 December 2007
Available online 9 January 2008

Abstract

Biomarkers are commonly used for verification of infection in conjunction with the development of viral vectors or experiments involving virus infection. Leukocyte surface antigens (CDs) are a prime option for biomarkers since they can be easily visualized and analyzed by flow cytometry after indirect fluorescent staining. For analyses of human cells, murine CD24 (Heat Stable Antigen: HSA) and CD90.2 (Thy-1.2) are currently being used. In the study reported here, we attempted to develop a rapid system for measuring retroviral genome recombination efficiency. For this purpose, we looked for an alternative CD molecule which could be used as a marker on a viral vector concurrently with other markers. We found that murine CD52 is suitable for this purpose because of its small gene size, low inhibitory effect on virus production, and measurable level of surface expression. With this novel biomarker, we succeeded in developing a rapid viral recombination measuring system using a flow cytometer.

Keywords: Retrovector; Biomarker; CD52; Recombination; Flow cytometry

1. Introduction

The use of retroviral vectors for gene delivery has become very common in recent years. To determine the efficiency of gene induction and/or to monitor the fate of induced cells, a variety of selectable markers have been incorporated into retroviral vectors. The genes of products that confer resistance to toxic compounds are widely used from the start of vector development, since their stable expression enables positive selection of cells induced by prolonged treatment with antibiotics [1]. Fluorescent proteins such as eGFP and RFP are widely used as markers because of their high stability, minimal toxicity, and non-invasive detection [2].

Cell surface molecules, such as leukocyte surface antigens (CDs), constitute another type of commonly used selectable marker antigens. Staining cells with fluorescent dye-conjugated antibodies and analyzing them with a flow cytometer enables the rapid and quantitative detection of transferred gene expression in the desired target cells while they are still alive. However, most of the genes used as selectable markers are relatively large, leaving limited space in the retroviral vector for other genes of interest. The human hematopoietic cell surface antigen CD24 and its murine homologue, the heat stable antigen (HSA), are two of the few exceptions because of their relatively small gene size (about 0.24 kb) and potential for cell surface expression. Because of these properties, CD24 and HSA are widely used as biomarkers [3,4]. Another surface antigen, CD90.2 (Thy-1.2), is also in common use as a biomarker although its gene size (488 bp) is larger than that of HSA [5].

To monitor retroviral infection and viral genome recombination in cells, several good vector assay systems have been developed [6,7]. Rhodes et al. described an attractive method using two similar vectors with mutated eGFPs and surface markers to measure their infectivity and recombination rate [8]. These systems are based on the principle that only a single

* Corresponding author. Department of Viral Infections, Research Institute for Microbial Diseases, Osaka University, 3-1 Yamadaoka, Suita City, Osaka 565-0871, Japan. Tel.: +81 6 6879 8348; fax: +81 6 6879 8347.
E-mail address: sakuragi@biken.osaka-u.ac.jp (J.-i. Sakuragi).

1286-4579/$ - see front matter © 2008 Elsevier Masson SAS. All rights reserved.
doi:10.1016/j.micinf.2007.12.016

DNA is formed in an infectious retroviral particle [9]. Although this system promises reasonable and stable results, it requires multiple cell sorting and expansion, so that it takes considerable time and effort to perform. In addition, the vectors carry IRES sequences for marker gene expression, sequences which do not exist in the native retroviral genome. We therefore wanted to modify this recombination assay system since we intended to evaluate HIV-1 genome recombination in a situation more similar to viral physiological conditions and to simplify the experiments. We attempted to generate retrovectors which could express two or more biomarkers at the same time for the development of the recombination assay system. Since it was therefore necessary to find a new biomarker, we explored the database and found that murine CD52 (mCD52), a protein of the CD24/HSA family, might have the characteristics required for our purpose.

2. Materials and methods

2.1. DNA constructs

The replication competent HIV-1 proviral clone pNL4-3 [10] and pMSMBA [11], a derivative of pNL4-3, were used as progenitors for the mutant constructs described below. The HSA gene was amplified from the plasmid pNLrHSAS [12], also a derivative of pNL4-3, the vpr gene of which was replaced with the HSA gene, with a pair of primers (XbaHSAonF: 5′-TCTAGAGCCGCCATGGGCAGAGCG-3′, and EcoRIHSAstpR: 5′-GAATTCTCTAACAGTAGAGATG-3′). pNLrHSAS was digested with NheI, blunt-ended with a Blunting-High kit (Toyobo, Osaka, Japan), and ligated to generate pNLrHSASNh. The amplified fragment was replaced with the XbaI-EcoRI region of pNLrHSASNh to add a Kozak sequence upstream of the ATG codon of the HSA gene to enhance its expression, and the resultant plasmid was named pNLrH. pNLrH was then digested with HpaI and XhoI, and the HpaI-XhoI fragment of pGEMHnGX [13] including the EGFP gene was inserted in the corresponding position to construct pNLrHnG.

The murine CD52 (mCD52) gene coding fragment was generated by synthesizing three oligonucleotide probes (CD52atg-95: 5′-ATGAAGAGCTTCCTCCTCTTCCTCAC TATCATTCTTCTGGTTGTGATTCAGATACAAACAGGAT CCTTGGGACAAGCCACTACGGCCGCTTCTGG-3′, CD52 cmpl170-116: 5′-GGCACCCGCATCGATGATGGATGAGG CCCCACTCTTTAAGGGGGTTTTTTTGGTGGAGGTGCTG TTTTTGTTAGTACCAGAAGCGGCCGTAGTGG-3′, and CD52fwd151-stp: 5′-CCATCATCGATGCGGGTGCCTGCAGTTT CCTCTTCTTTGCCAATACCTTAATGTGCCTCTTCTACC TCAGCTGA-3′) following sequential PCR amplification with two pairs of primers (XbaKozCD52F: 5′-TCTAGAGCCGC CATGAAGAGCTTCCTCCTCTTCC-3′, CD52RevCla: 5′-GG CACCCGCATCGATGATGGATG-3′, CD52FwdCla: 5′-CCAT CATCGATGCGGGTGCCTGC-3′, and CD52RevStp: 5′-TCA GCTGAGGTAGAAGAGGCAC-3′). The 0.23 kb amplified fragment was purified, ligated to the pGEMTeasy vector (Promega, Madison, WI) to construct pGEMmCD52, and verified for its sequence authenticity. pNLrHnG was digested with XbaI and EcoRI, and the XbaI and EcoRI fragment of pGEMmCD52, including the mCD52 gene, was inserted at the corresponding position to construct pNLrCnG. A base substitution mutation was then introduced into the start codon of the eGFP gene of pNLrHnG to eliminate eGFP expression (ATG to TAA) in order to allow for the construction of pNLrHnGΔN. A frame shift mutation of the eGFP gene at the 0.6 kb position from the start codon was introduced as reported elsewhere [8] (mutant pON-H6: one-base substitution and one-base insertion to introduce a stop codon and a frame shift) into pNLrCnG for the construction of pNLrCnGΔC. Furthermore, two-base substitution mutation at the hairpin loop of SL1 (GCGCGC to GTGCAC) was introduced into pNLrCnGΔC to construct SL1MrCnGΔC.

2.2. DNA transfection

293T cells [14] (approximately 3×10^6) were seeded on dishes (diameter 100 mm) the day before transfection with plasmid DNA (total 5 μg) using the calcium phosphate precipitation method [15]. The day after transfection, the supernatant was replaced with fresh medium.

2.3. Virus infection

At 48–72 h post-transfection, the media was centrifuged and the supernatant was used for infection into T-cell lines (MT-4 and M8166).

2.4. RT-PCR assay

Two days after transfection, 293T cells were harvested and total cellular RNA was extracted with TRIzol (Invitrogen, Carlsbad, CA). RNAs were treated with RQ1-DNaseI (Promega) for removal of contaminated DNAs. Reverse transcription (RT) reaction using 5 μg of total RNA with Superscript III (Invitrogen) was performed according to the manufacturer's instructions, and one-twentieth of the RT products was used for the PCR template. Two sets of primer pairs were prepared to detect the mCD52 gene (Forward: 5′-TCTAGAGCCGC CATGAAGAGCTTCCTCCTCTTCC-3′; reverse: 5′-TCAGC TGAGGTAGAAGAGGCAC-3′) and the GAPDH gene (forward: 5′-CCACATCGCTCAGACACCAT-3′; reverse: 5′-GGC AACAATATCCACTTTACCAGAGT-3′). Amplified products were subjected to agarose gel electrophoresis and visualized by means of ethidium bromide staining.

2.5. Flow cytometric analysis

Mock-infected cells, an empty vector, and HSA/eGFP/mCD52/Thy-1.2-infected cell populations in growth medium were first centrifuged and washed twice in PBS(−) supplemented with 10% Blocking One solution (Nacalai Tesque Inc., Kyoto, Japan). Aliquots of the cells were then stained with an anti-mCD52 rat monoclonal antibody (MBL Co. Ltd., Nagano, Japan) for 30 min, washed twice, incubated with Allophycocyanin (APC)-labeled anti-rat Ig polyclonal

antibody (BD Biosciences, San Jose, CA) for an additional 30 min, and washed twice. The cells were then stained with directly conjugated anti-murine HSA-Phycoerythrin (PE) antibody and anti-murine Thy-1.2-biotin antibody (both from BD Biosciences) for an additional 30 min, washed twice, and stained with PerCP-Cy5.5-conjugated Streptavidin (BD Biosciences). After antibody labeling, two further washes in PBS(−) were performed, the last together with 1% formaldehyde to fix the cells. Finally, the cells were analyzed on a FACSCalibur (BD Biosciences).

3. Results

3.1. Generation of mCD52 expressing HIV-1 vectors

To construct multi-marker carrying retrovectors, we initially tried to use the existing biomarkers. Within the HIV-1 genome, the vpr, env, and nef coding regions were replaced with HSA, Thy-1.2, and eGFP genes in various combinations. While the HSA gene was well expressed under any conditions, the Thy-1.2 and eGFP genes performed well only when located within the nef coding region (data not shown). Any vector carrying the Thy-1.2 or eGFP gene in the vpr or env region produced little or no viral particles. Hence, we needed to find a novel marker with approximately the same potential as CD24/HSA and that could be used concurrently with them.

Human and murine CD52s (h/mCD52) belong to a group of very small GPI-anchored sialoglycoproteins which include CD24/HSA and with size and protein properties resembling those of CD24. Human CD52 is abundantly expressed on lymphocytes and monocytes, and is also expressed in non-lymphoid tissue in epithelial cells of the distal epididymal and deferent ducts from which it is transferred to the surface of sperm [16]. The gene size of mCD52 is only 222 bp and encodes 74 peptides (Fig. 1A). A computer search found no significant homology of mCD52 to any known molecules except hCD52 at either the DNA or amino acid sequence level [17]. Although it retains a certain homology to hCD52 within the N- and C-terminal signal region, the amino acid sequence of the mature peptide region of mCD52 is significantly different from that of its human homologue [16]. In addition, it has been suggested that the monoclonal antibody BTG-2G, which is the only commercially available anti-mCD52 monoclonal antibody (mAb) [17], can recognize peptides containing KKTPL [18]. This sequence is unique to mCD52 (Fig. 1A) and thus no cross-reaction of the antibody with hCD52 can be expected. These characteristics suggested to us that mCD52 could be a candidate for a novel selectable marker of gene transfer in human cells. We cloned the mCD52 gene by synthesizing and amplifying its DNA primers and inserting it in place of the vpr gene of HIV-1 to construct various retrovectors. Fig. 1B shows representative schematics of the vectors we constructed for the experiments described below. We confirmed expression of the mCD52 gene by means of an RT-PCR assay (Fig. 1C). A transcription of the mCD52 gene was clearly detected in cells transfected with the vectors carrying the mCD52 gene. The production of the viral antigen from cells transfected with vectors carrying the mCD52 insertion was only moderately reduced compared to that from cells transfected with the wild-type or the vectors carrying HSA (data not shown). This indicated that the effect of mCD52 insertion into the viral genome on virus production was nearly negligible.

3.2. Detection of cell surface expression of mCD52 by mAb

We first used a flow cytometer to verify surface expression of the mCD52 protein and its detection with an mAb. 293T cells were then transfected with pNLrCnG, which carries both the mCD52 and eGFP genes as biomarkers. Two plasmids, pNLNh and pNLrHnG, were used for transfection as parallel controls. Unlike pNLrCnG, pNLrHnG carries an HSA gene instead of an mCD52 gene. Forty-eight hours after transfection, the cells were stained with anti-mCD52 mAb, APC-anti-RatIg antibody, and phycoerythrin (PE)-conjugated anti-HSA mAb. The cells were fixed with 1% formaldehyde-containing PBS(−), and analyzed with a flow cytometer. The expressions of eGFP, HSA, and mCD52 were detected through channels FL1, FL2, and FL4, respectively. The results showed good expression and separation of the three marker genes (Fig. 1D), suggesting that these markers could be utilized concurrently within a cell for discrimination of their expression. Double marker positive cells accounted for about 11% (NLrCnG) and 14% (NLrHnG) of total cells.

3.3. Four-color analysis of transduced cells using three surface markers and eGFP

As expression of mCD52 was clearly distinguishable from the expressions of HSA and eGFP, we attempted to identify gene transductions mediated by multiple retrovectors by means of four biomarkers using all fluorescence channels (FL1–4) of a flow cytometer. For this purpose, the vectors pNLrCnGΔC (NLC) and pNLrHnGΔN (NLH) were prepared. NLC carries the mCD52 gene and NLH the HSA gene, and both carry inactivated eGFP genes. In addition, another surface marker gene, murine Thy-1.2, was employed for analysis. The vector pNLΔBgThy [5] (NLT) carries the Thy-1.2 gene in place of the nef gene, features deletion of the Env gene of pNL4-3 and does not carry the eGFP gene. Biotin-conjugated anti-Thy-1.2 mAb and Avidin-PerCP-Cy5.5 were used for staining and labeling Thy-1.2. The order of cell staining is shown in Fig. 2A. 293T cells were transfected with pCG-VSVG and various combinations of retrovectors. Two days post-transfection, the cells and supernatants were harvested, and the cells were stained with the mAbs and analyzed with a flow cytometer (data not shown). As expected, four biomarkers were detected independently and no cross-reaction was observed. The harvested supernatants were then used for the infection assay with MT-4 cells (Fig. 2B). Similar to the finding for 293T, infection of retrovectors resulted in a satisfactory expression and detection of marker genes with a flow cytometer. The bottom row of the panel in Fig. 2B shows

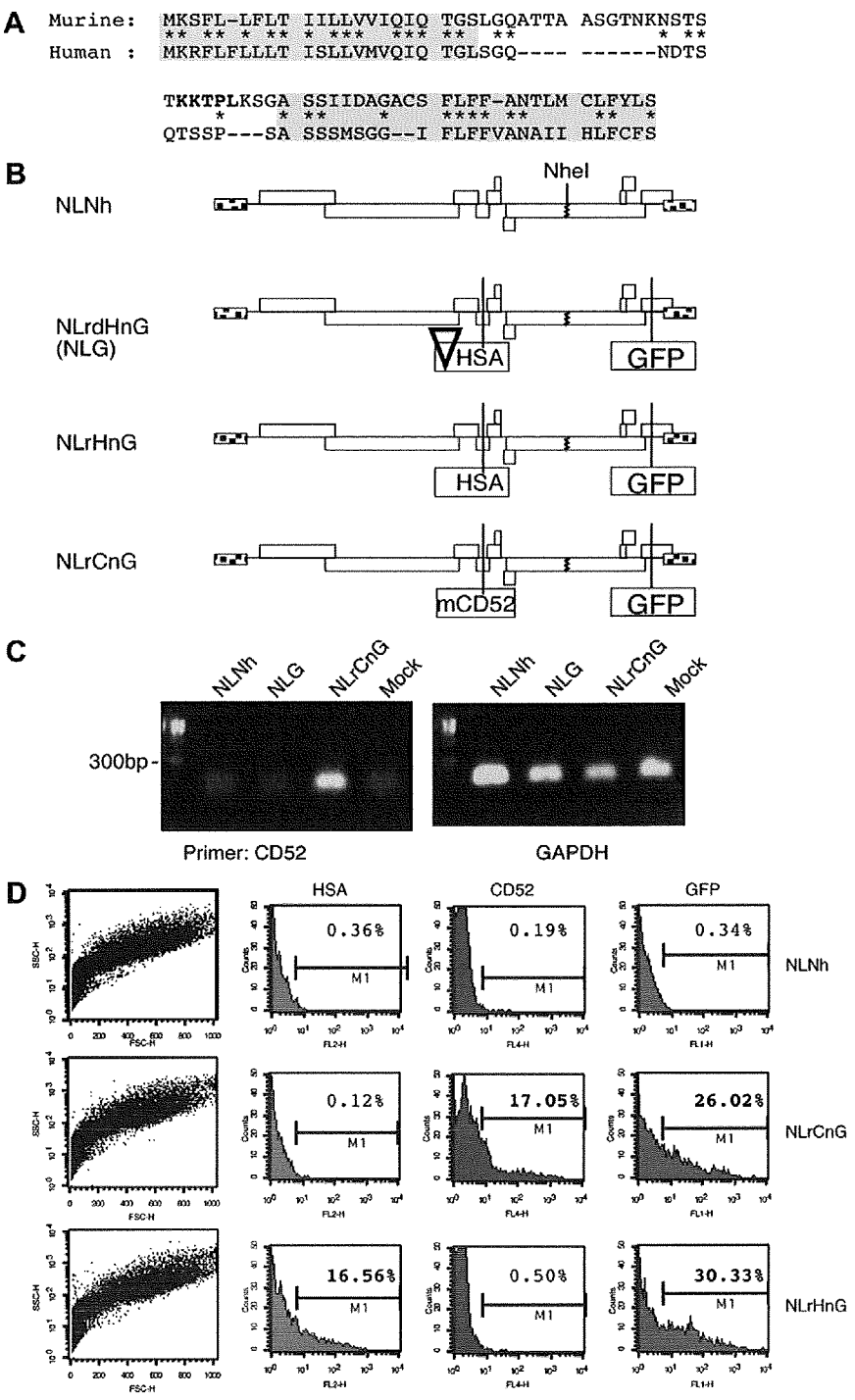

Fig. 1. Construction of murine CD52 expressing HIV-1 vector. A) Comparison of murine and human CD52 protein sequences. N-terminus signal sequences and C-terminus GPI-addition sequences [22] are shaded. The BTG-2G monoclonal antibody recognition sequence [18] are shown in bold. B) Schematic of constructed HIV-1 vectors. Plain boxes represent ORFs of HIV-1 genes and stippled boxes represent LTRs. The env gene in each vector was inactivated by frameshift mutation introduced at the NheI site. The boxes labeled HSA, GFP, and mCD52 represent marker genes inserted in the vectors. The triangle represents the location of mutations introduced to inactivate the gene. C) RT-PCR assays to confirm mCD52 expression. 293T cells were transfected with the plasmids shown in Fig. 1B. Cells were harvested 2 days post transfection and total cellular RNA was extracted. RT products of 5 μg of total cellular RNA were used for PCR amplification. Detection of the expression of the GAPDH gene was used for control. Faint signals for mCD52 in control lanes were non-specific since they also appeared in RT negative controls (data not shown). D) Surface expression of mCD52 molecules caused by transfection. 293T cells were transfected, harvested, and stained with anti-mCD52 Rat monoclonal antibody, APC-conjugated anti-Rat IgG antibody, and PE-conjugated anti-HSA monoclonal antibody. Four charts in one row represent one set of analyses of one sample. Plasmids used for transfection and molecules detected by cytometric analysis are indicated to the left of the rows and above the columns respectively. Percentages of positive cells are shown in each histogram.

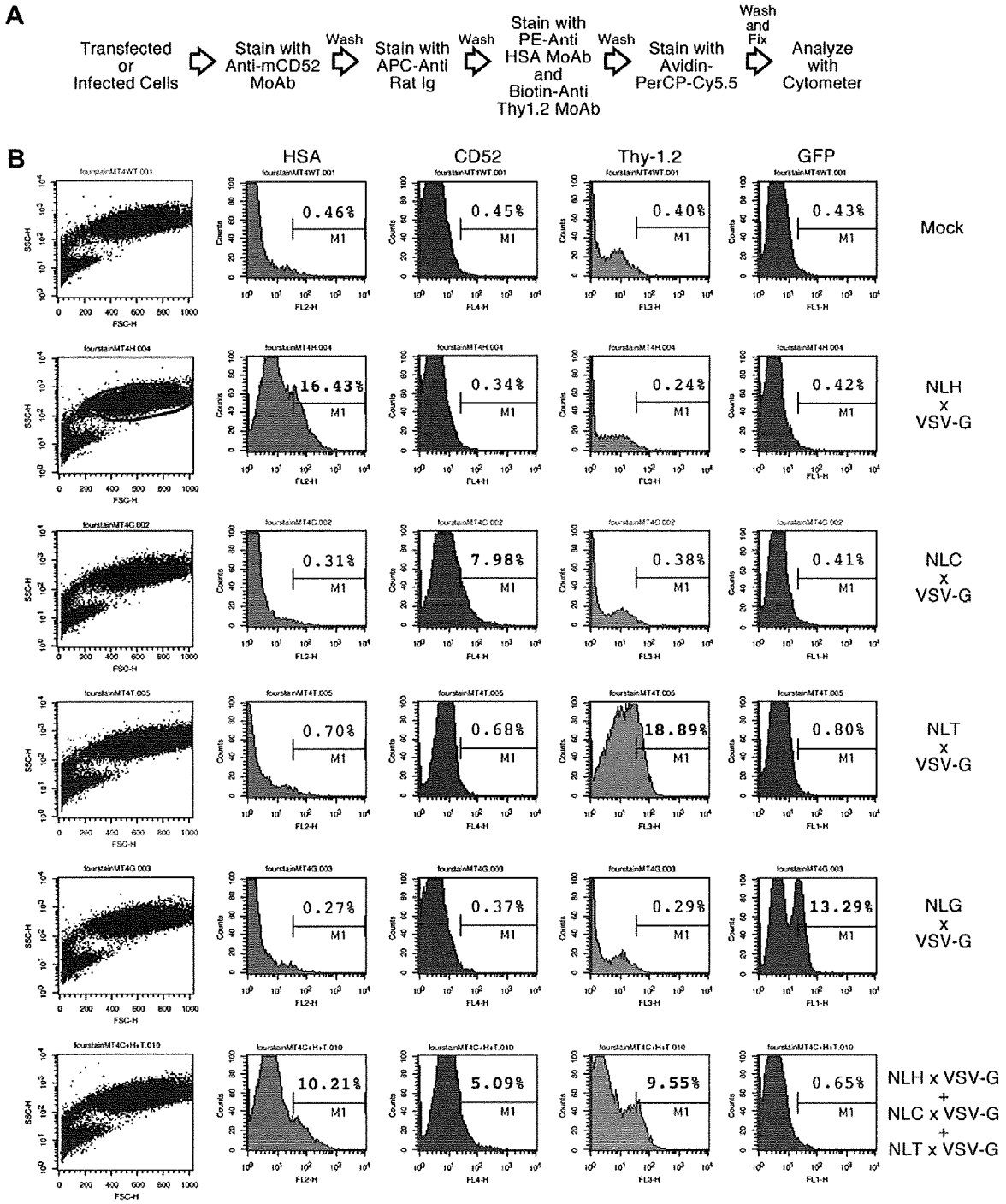

Fig. 2. Simultaneous detection of four biomarkers transduced by retrovectors. A) Flowchart of cell staining of the assay. B) MT-4 cell infection experiment. The supernatants of 293T cells transfected with pCG-VSVG and various retrovectors were collected and used for infection into MT-4. Six charts in one row represent one set of analyses of one sample. The notations are the same as those for Fig. 1D. The "x" between two or three plasmids indicates co-transfection of the plasmids.

that co-infection of the mixture of three vectors resulted in a lack of eGFP expression, thus indicating that no recombination between GFPΔN and GFPΔC from different virus particles had occurred. We therefore proved that these three surface markers could be conveniently leveraged to distinguish the gene induction of different vectors simultaneously, and that their utilization could be expected to have a wide range of applications.

3.4. Construction of HIV-1 genome recombination assay

We then attempted to develop a simple system to monitor retroviral infection and viral genome recombination in cells. The system we designed is shown in Fig. 3. Two similar vectors with the same or different dimerization signals (DLS) were constructed (Fig. 3A) and co-transfected together with or without the VSV-G expression vector (pCG-VSVG) (Fig. 3B). Vector A carries a surface biomarker (Mark-A) and an inactivated eGFP gene with amino-terminal mutation (GFPΔN), while vector B carries another biomarker (Mark-B) and an inactivated eGFP gene with carboxyl-terminal mutation (GFPΔC). After transfection, the released virions can be

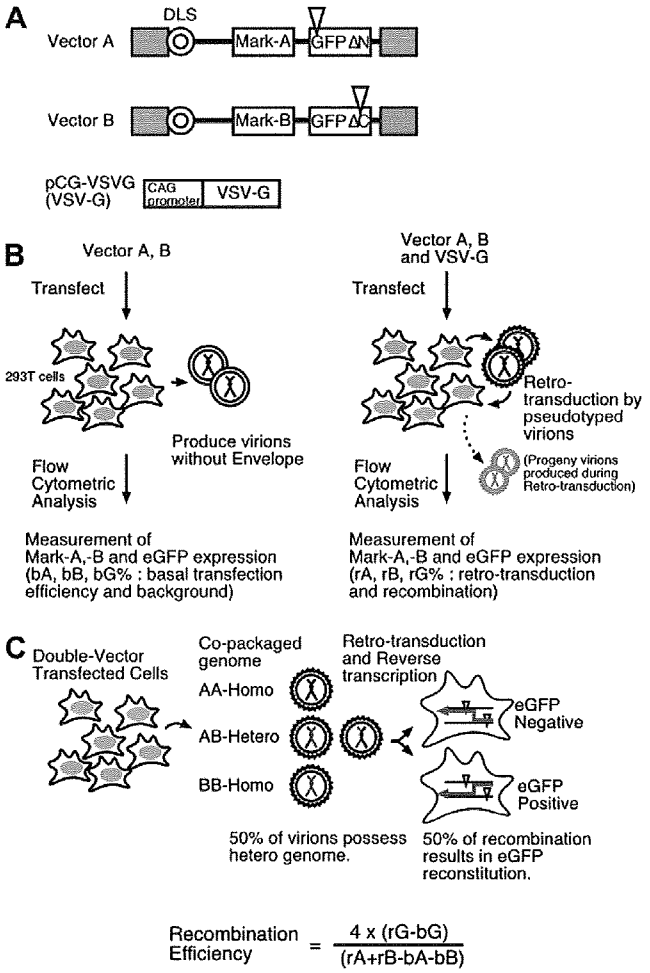

Fig. 3. The system for estimating HIV-1 recombination efficiency using retro-transduction realized by means of pseudotyping. A) Schematics of the vectors planned for the system. Symbols are the same as those for Fig. 1B. Concentric circles represent encapsidation/dimerization signals (E/DLS). B) Experimental design of the system. Without VSV-G, co-transfection of the vectors results in production of non-infectious virions and expression of marker genes (left). With VSV-G pseudotyping, the generated virions infect the cells within the transfected cell culture (retro-transduction), and marker gene expressions are enhanced. C) Estimation of recombination efficiency. Co-transfected cells produce 25% A-A and 25% B-B homo-dimerized genomes, as well as 50% A-B hetero-dimerized genomes containing virions. Fifty % of the opportunity for genome recombination results in reconstitution of the eGFP gene.

expected to co-package the homo- or hetero-dimerized vector genome, while the ratio of homo- to hetero-dimerization should be one-to-one if the genome expression efficiency of the two vectors is similar (Fig. 3C). Without VSV-G, the expression of Mark-A and -B indicates transfection efficiency of the vectors, and no eGFP expression should be observed. With VSV-G expression, pseudotyped virions have been observed to cause retro-transduction to the producer cells [13] and the number of marker genes expressing cells in the transfectant increases with an increase in the occurrence of retro-transduction. Recombination of the two vectors can be assumed to occur only in retro-transduced cells, and is monitored in terms of further restoration and expression of the eGFP gene (Fig. 3C). Transfection and retro-transduction efficiency are measured by expression of Mark-A and -B, while the transduction efficiency is estimated by subtracting marker gene expression ratios of the VSV-G negative sample (bA, bB%) from those of the positive sample (rA, rB%). Finally, the recombination efficiency is estimated by calculating the ratio of eGFP expressing cells (rG−bG%) in vector-transduced cells. If we assume that one of the recombination events always occurs between the ΔN and ΔC mutation of eGFPs during reverse transcription, 50% of the recombination events should result in reconstitution of the eGFP gene. In addition, 50% of the virions from doubly transfected cells possess a hetero-dimerized genome, and thus have the potential to reconstitute eGFP. This means that a ratio of eGFP positive cells of 25% in Mark-A or -B positive cells should be the maximum value for recombination. We therefore adopted this maximum ratio for easy indexing by quadrupling the numeric results (Fig. 3C).

We assessed the efficacy of this system by constructing and testing several vectors derived from HIV-1. We found that the combination of vpr substitution with HSA or mCD52 as surface markers and nef substitution with mutated eGFP genes yielded satisfactory results in terms of virion production, infectivity, and marker expression. We also used this system to verify the recombination between the wild-type retrovectors and those derived from a dimerization initiation site (DIS) mutant of HIV-1 (Fig. 4). DIS is located in DLS and it has been suggested that it performs core functions in viral genome recombination [19]. The vectors NLC and NLH carry the same DIS, whereas pSL1MrCnGΔC (SL1MC) carries a two-base substitution on DIS (Fig. 4A), so that heterogenome dimer formation between NL- and SL1M-vectors can be assumed to be reduced. In this experiment (Fig. 4B), 3–5% of all cells were surface marker positive cells in non-pseudotyped samples (NLH × NLC, NLH × SL1MC), which constitutes evidence of the efficiency of transfection and marker expression. eGFP fluorescence was not detected in these samples, confirming that ΔN or ΔC mutation inactivated the functional eGFP expression. In contrast, HSA/mCD52 expression was dramatically enhanced by about 80% in pCG-VSVG co-transfected samples due to retro-transduction. Efficient reconstitution of eGFP was observed in the homo-DIS sample (20% of total cells) whereas only limited eGFP expression was detected in the hetero-DIS sample (4%), thus indicating diminished occurrence of recombination as also reported elsewhere [19]. Recombination efficiency was

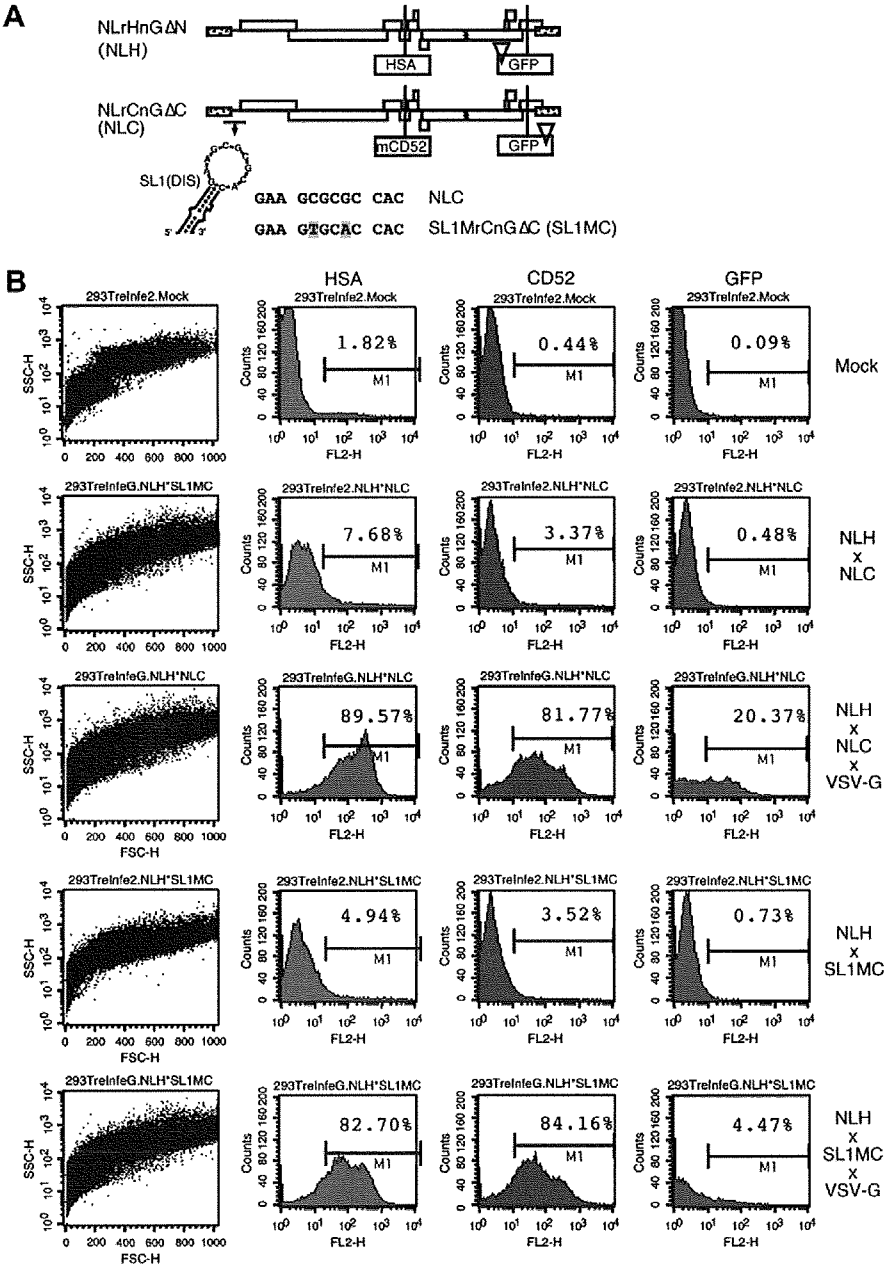

Fig. 4. Detection of HIV-1 recombination. A) Schematic of the vectors actually constructed for the recombination estimation system. Two nucleic acids on DIS of pNLrCnGΔC were substituted for each other (5′-GCGCGC-3′ for 5′-GTGCAC-3′) to construct pSL1MrCnGΔC. B) Genome recombination assay using 293T cells. The notations are the same as those for Fig. 2B.

estimated at 0.5 for NL-NL [4(20.37 − 0.48)/(89.57 + 81.77 − 7.68 − 3.37) = 0.496] and 0.09 for NL-SL1M [4(4.47 − 0.73)/(82.70 + 84.16 − 4.94 − 3.52) = 0.094]. The efficiency of heterogenome dimerization between NL and SL1M mutant estimated with the system devised by us [20] was reduced to about 30% of that of homo-dimerization (data not shown), which suggests there is a parallel interrelation between genome dimerization and recombination. These results clearly showed that our system utilizing retro-transduction is effective and quite practical for evaluation of recombination.

4. Discussion

In this report, we described the practical use of a new reporter gene, mCD52, and the development of a rapid recombination assay system for HIV-1. We focused on the mCD52, which is a protein of the HSA family, since its gene is as small as that of HSA and was assumed to possess similar properties. The results of our study demonstrated that mCD52 can be a useful biomarker since its insertion into the vpr region resulted in its expression from the HIV-1 genome similar to that of HSA.

The recombination assay system we developed is relatively simple, easy and fast. Infection to the transfected cells (=retro-transduction) is the key component of the system, and without it, this system cannot be operated. Retro-transduction is inevitable as far as using the VSV-G protein for pseudotyping, since the VSV-G pseudotyped vector can infect virtually any kind of cell [13]. On the other hand, it is not easy to attain high enough infectivity of the vectors to calculate the recombination rate without VSV-G. We therefore constructed this system with VSV-G by taking advantage of retro-transduction for a quick estimation. For reliability of the calculation, however, the efficiency of retro-transduction is a matter of concern. If the titer of the vectors is too high, multiple infections would occur in a single cell. As the estimate of the recombination rate is based on the assumption of a "single-hit" infection per cell, too high an efficiency of vector production might bias the estimate. In several reports, the recombination frequency of HIV-1 in cultured cells is estimated at about once per 0.9–1 kb of viral genome [6,8]. Our result for the normal recombination rate was 0.5 times per 0.6 kb, so that the estimated frequency is once per 1.2 kb. Since this value represents a lower efficiency than previously reported, it may be the result of multiple infections reflecting a high infection rate (most of the cells in the culture were marker positive as seen in Fig. 4). To prevent biased estimates, a reduction in vector infectivity is needed for this system. In fact, when we reduced the titer of the vector appropriately to minimize "multiple-hit" infection, the calculated recombination ratio was as one event per 0.8 kb, which was very close to the previously published data (data not shown).

There is a possibility that viral genome-derived cDNA and transfected plasmid DNA recombine in retro-transduced cells. We performed an additional experiment to verify this possibility. The 293T cells were cotransfected with the plasmid NLH, pCG-VSVG, and the plasmid carrying only GFPΔC gene. After three-day incubation, we observed no appearance of GFP positive cells in retrotransduced cell culture, whereas a certain number of HSA positive cells appeared (data not shown). This clearly showed that the recombination between the GFPΔN gene derived from viral cDNA and the GFPΔC gene derived from the transfected plasmid was undetectable during retro-transduction. Thus, we believe that plasmid-cDNA recombination is negligible in this system. Like in other established systems [6,8], the recombination rate estimated by our system only reflects that in the nef coding region. By changing the structure of the vectors, it may be possible to further study the recombination rate in regions other than the nef region.

We did not encounter any practical problems such as alterations of cell viability caused by the expression and staining of mCD52. Specific mAb (Campath-1H) treatment of human CD52 has been shown to lead to extensive eradication of CD52 positive cells by complement activation and is thus utilized for bone marrow transplantation therapy [21]. Although our system includes anti-mCD52 mAb treatment, the mAb we used was different from Campath-1H, and the treatment of cells in our study lasts only for a short time prior to cell fixation. In addition, complement components in cell culture media were inactivated by heat inactivation of serum. Although mCD52 seemed to cause no serious defects in the experiment, mCD52 expression may have some deleterious effect under certain conditions such as in *in vivo* experiments. The potential problems associated with wider application of our system thus need to be investigated.

In conclusion, mCD52 constitutes a novel option for a reporter gene which can be leveraged concurrently with other biomarkers. We could demonstrate that mCD52 is a useful marker for transduction by retrovectors, and the utility of this system may be extended to various viral and non-viral gene transfer systems. With this new marker, we developed an easy-to-use HIV-1 recombination assay system, which is expected to be useful for studying and determining the recombination ratios of many viral strains and/or mutants at one and the same time.

Acknowledgements

This work was supported by grants from the Ministry of Education, Culture, Sports, Science and Technology, the Ministry of Health, Labour, and Welfare, and the Health Science Foundation, Japan.

References

[1] C. Karreman, A new set of positive/negative selectable markers for mammalian cells, Gene 218 (1998) 57–61.
[2] P. van Roessel, A.H. Brand, Imaging into the future: visualizing gene expression and protein interactions with fluorescent proteins, Nat. Cell Biol. 4 (2002) E15–E20.
[3] R. Pawliuk, R. Kay, P. Lansdorp, R.K. Humphries, Selection of retrovirally transduced hematopoietic cells using CD24 as a marker of gene transfer, Blood 84 (1994) 2868–2877.
[4] E. Conneally, P. Bardy, C.J. Eaves, T. Thomas, S. Chappel, E.J. Shpall, R.K. Humphries, Rapid and efficient selection of human hematopoietic cells expressing murine heat-stable antigen as an indicator of retroviral-mediated gene transfer, Blood 87 (1996) 456–464.
[5] V. Planelles, A. Haislip, E.S. Withers-Ward, S.A. Stewart, Y. Xie, N.P. Shah, I.S. Chen, A new reporter system for detection of retroviral infection, Gene Ther. 2 (1995) 369–376.
[6] D.N. Levy, G.M. Aldrovandi, O. Kutsch, G.M. Shaw, Dynamics of HIV-1 recombination in its natural target cells, Proc. Natl. Acad. Sci. U.S.A. 101 (2004) 4204–4209.
[7] A. Onafuwa, W. An, N.D. Robson, A. Telesnitsky, Human immunodeficiency virus type 1 genetic recombination is more frequent than that of Moloney murine leukemia virus despite similar template switching rates, J. Virol. 77 (2003) 4577–4587.
[8] T.D. Rhodes, O. Nikolaitchik, J. Chen, D. Powell, W.S. Hu, Genetic recombination of human immunodeficiency virus type 1 in one round of viral replication: effects of genetic distance, target cells, accessory genes, and lack of high negative interference in crossover events, J. Virol. 79 (2005) 1666–1677.
[9] J. Coffin, S. Hughs, H. Varmus (Eds.), Retroviruses, Cold Spring Harbor Laboratory Press, New York, 1997.
[10] A. Adachi, H.E. Gendelman, S. Koenig, T. Folks, R. Willey, A. Rabson, M.A. Martin, Production of acquired immunodeficiency syndrome-associated retrovirus in human and nonhuman cells transfected with an infectious molecular clone, J. Virol. 59 (1986) 284–291.
[11] M.S. McBride, A.T. Panganiban, The human immunodeficiency virus type 1 encapsidation site is a multipartite RNA element composed of functional hairpin structures, J. Virol. 70 (1996) 2963–2973.

[12] B.D. Jamieson, J.A. Zack, In vivo pathogenesis of a human immunodeficiency virus type 1 reporter virus, J Virol. 72 (1998) 6520–6526.
[13] M. Ohishi, T. Shioda, J.I. Sakuragi, Retro-transduction by virus pseudotyped with glycoprotein of vesicular stomatitis virus, Virology 362 (2007) 131–138.
[14] F.L. Graham, J. Smiley, W.C. Russell, R. Nairn, Characteristics of a human cell line transformed by DNA from human adenovirus type 5, J. Gen. Virol. 36 (1977) 59–74.
[15] A. Aldovini, B.D. Walker, Techniques in HIV Research, Stockton Press, New York, 1990.
[16] M. Tone, K.F. Nolan, L.A. Walsh, Y. Tone, S.A. Thompson, H. Waldmann, Structure and chromosomal location of mouse and human CD52 genes, Biochim. Biophys. Acta 1446 (1999) 334–340.
[17] H. Kubota, H. Okazaki, M. Onuma, S. Kano, M. Hattori, N. Minato, Identification and gene cloning of a new phosphatidylinositol-linked antigen expressed on mature lymphocytes. Down-regulation by lymphocyte activation, J. Immunol. 145 (1990) 3924–3931.
[18] G. Hale, Synthetic peptide mimotope of the CAMPATH-1 (CD52) antigen, a small glycosylphosphatidylinositol-anchored glycoprotein, Immunotechnology 1 (1995) 175–187.
[19] M.P. Chin, T.D. Rhodes, J. Chen, W. Fu, W.S. Hu, Identification of a major restriction in HIV-1 intersubtype recombination, Proc. Natl. Acad. Sci. U.S.A. 102 (2005) 9002–9007.
[20] J. Sakuragi, S. Ueda, A. Iwamoto, T. Shioda, Possible role of dimerization in human immunodeficiency virus type 1 genome RNA packaging, J. Virol. 77 (2003) 4060–4069.
[21] A. Domagala, M. Kurpisz, CD52 antigen–a review, Med. Sci. Monit. 7 (2001) 325–331.
[22] M.Q. Xia, G. Hale, M.R. Lifely, M.A. Ferguson, D. Campbell, L. Packman, H. Waldmann, Structure of the CAMPATH-1 antigen, a glycosylphosphatidylinositol-anchored glycoprotein which is an exceptionally good target for complement lysis, Biochem. J. 293 (Pt 3) (1993) 633–640.

blood

2008 111: 243-250
Prepublished online Sep 24, 2007;
doi:10.1182/blood-2007-04-086017

Interaction between Hck and HIV-1 Nef negatively regulates cell surface expression of M-CSF receptor

Masateru Hiyoshi, Shinya Suzu, Yuka Yoshidomi, Ranya Hassan, Hideki Harada, Naomi Sakashita, Hirofumi Akari, Kazuo Motoyoshi and Seiji Okada

Blood (print ISSN 0006-4971, online ISSN 1528-0020), is published semimonthly by the American Society of Hematology, 1900 M St, NW, Suite 200, Washington DC 20036.

Interaction between Hck and HIV-1 Nef negatively regulates cell surface expression of M-CSF receptor

Masateru Hiyoshi,[1] Shinya Suzu,[1] Yuka Yoshidomi,[1] Ranya Hassan,[1] Hideki Harada,[1] Naomi Sakashita,[2] Hirofumi Akari,[3] Kazuo Motoyoshi,[4] and Seiji Okada[1]

[1]Division of Hematopoiesis, Center for AIDS Research; [2]Department of Cell Pathology, Graduate School of Medical and Pharmaceutical Sciences, Kumamoto University, Kumamoto; [3]Laboratory of Disease Control, Tsukuba Primate Research Center, National Institute of Biomedical Innovation, Ibaraki; and [4]Third Department of Internal Medicine, National Defense Medical College, Saitama, Japan

Nef is a multifunctional pathogenetic protein of HIV-1, the interaction of which with Hck, a Src tyrosine kinase highly expressed in macrophages, has been shown to be responsible for the development of AIDS. However, how the Nef-Hck interaction leads to the functional aberration of macrophages is poorly understood. We recently showed that Nef markedly inhibited the activity of macrophage colony-stimulating factor (M-CSF), a primary cytokine for macrophages. Here, we show that the inhibitory effect of Nef is due to the Hck-dependent down-regulation of the cell surface expression of M-CSF receptor Fms. In the presence of Hck, Nef induced the accumulation of an immature under–N-glycosylated Fms at the Golgi, thereby down-regulating Fms. The activation of Hck by the direct interaction with Nef was indispensable for the down-regulation. Unexpectedly, the accumulation of the active Hck at the Golgi where Nef prelocalized was likely to be another critical determinant of the function of Nef, because the expression of the constitutive-active forms of Hck alone did not fully down-regulate Fms. These results suggest that Nef perturbs the intracellular maturation and the trafficking of nascent Fms, through a unique mechanism that required both the activation of Hck and the aberrant spatial regulation of the active Hck. (Blood. 2008;111:243-250)

Introduction

HIV-1 infections lead to the development of AIDS by causing progressive degeneration of the immune system.[1-3] The main cellular targets of HIV-1 are CD4$^+$ T cells and macrophages, and the depletion of CD4$^+$ T cells caused by an infection is suggested to account for many aspects of the pathogenesis of HIV-1.[1-3] Meanwhile, a number of studies have revealed the functional aberration of HIV-1–infected macrophages.[4,5] Infected macrophages showed an altered profile of the production of cytokine/chemokines[4] or migratory capacity,[5] which might contribute to the uncontrolled homeostasis of the immune system. Indeed, functional analyses of HIV-1 Nef protein have revealed that macrophages as well as CD4$^+$ T cells play an important role in the development of AIDS.

Nef is a 25- to 30-kDa protein with no enzymatic activity encoded by the HIV-1 genome.[6,7] Studies of HIV-1–infected patients have clearly demonstrated Nef to be a critical determinant of the development of AIDS: HIV-1 strains without an intact Nef gene were frequently isolated from nonprogressive long-term survivors.[8,9] Subsequent study of HIV-1 transgenic mice confirmed the pathogenetic activity of Nef: targeted expression of the entire coding sequence of HIV-1 in CD4$^+$ T cells and macrophages caused a severe AIDS-like disease in mice, which was completely abolished by the disruption of the Nef gene.[10] Importantly, only an amino acid substitution in the proline-rich (PxxP) motifs of Nef was sufficient to protect mice from the development of AIDS-like disease.[11] A number of studies have revealed that Nef interacts with a subset of cellular Src family tyrosine kinases, via the PxxP motifs.[12-15] The Nef PxxP motifs had an affinity for the Src homology (SH3) domain of Hck, Lyn, and possibly c-Src, but not of Fgr, Fyn, Lck, and Yes.[12-15] In particular, the interaction between the Nef PxxP motifs and the Hck SH3 domain was likely to be important, because the interaction caused the activation of Hck.[13-15] Indeed, a study with HIV-1 transgenic mice clearly demonstrated the importance of the Nef-Hck interaction for the development of AIDS: the appearance of the AIDS-like disease was significantly delayed when the HIV-1 transgenic mice expressing an intact Nef gene were crossed with an *hck*$^{-/-}$ background.[11] Given that Hck is expressed in macrophages but not in CD4$^+$ T cells,[16] the finding indicates that the Nef-Hck interaction in macrophages is at least in part responsible for the development of AIDS. However, little is known of the molecular mechanisms by which the Nef-Hck interaction contributes to the functional aberration of macrophages and the development of AIDS. The fact that Src kinases including Hck have both positive and negative roles in cell signaling pathways[16-19] makes it difficult to predict the functional consequences of the Nef-Hck interaction.

A well-characterized function of Nef is the down-regulation of the cell surface expression of CD4[6,7,20] or major histocompatibility complex class I (MHC I).[6,7,21-23] Nef accelerates the endocytosis of CD4,[20] the receptor for HIV-1,[1-3] which allows an efficient viral release from the host cells.[6,7] Nef reduces the level of the surface expression of MHC I through multiple mechanisms,[21-23] which diminishes the recognition of the infected cells by cytotoxic T cells.[6,7] However, these hallmark functions of Nef may not fully account for the functional significance of the Nef-Hck interaction,

Submitted April 17, 2007; accepted September 18, 2007. Prepublished online as *Blood* First Edition paper, September 24, 2007; DOI 10.1182/blood-2007-04-086017.

The online version of this article contains a data supplement.

The publication costs of this article were defrayed in part by page charge payment. Therefore, and solely to indicate this fact, this article is hereby marked "advertisement" in accordance with 18 USC section 1734.

because the down-regulation of CD4 or MHC I occurs even in the absence of Hck (ie, in $CD4^+$ T cells).[20-23] Meanwhile, we and others have recently identified the functions of Nef that are dependent on Hck.[24-26] Drakesmith et al demonstrated that Nef down-regulated the surface expression of HFE, an iron homeostasis regulator expressed on macrophages, which was abolished by a dominant-negative Hck.[24] Briggs et al demonstrated that Nef mimicked the cell growth–promoting activity of granulocyte-macrophage colony-stimulating factor (GM-CSF), a cytokine that supports the proliferation and differentiation of monocyte/macrophages,[27] possibly through a mechanism that required Hck and the Stat3 transcription factor.[25] Nef might contribute to the survival of macrophages by mimicking GM-CSF receptor pathways, allowing long-term viral replication.[25] In contrast to the latter finding, we demonstrated that Nef inhibited the growth of human myeloid leukemia TF-1-fms cells mediated by macrophage colony-stimulating factor (M-CSF),[26] another cytokine essential for the proliferation and differentiation of monocytes/macrophages.[28] The growth inhibition of the cells correlated well with the impaired activation of the M-CSF receptor Fms,[26] which is a tyrosine kinase encoded by the proto-oncogene *c-fms*.[28] Impaired activation of Fms was also observed in human embryonic 293 cells coexpressing Nef and Hck, but not in cells expressing Nef alone or Hck alone.[26] Thus, these data indicated that Nef inhibited the activation of Fms through a mechanism that required Hck.

The functions of macrophages are distinctly regulated by M-CSF and GM-CSF,[27,28] as evidenced by the marked difference in the morphology of macrophages derived from these cytokines.[29] Moreover, these macrophages showed different profiles of the production of chemokines/cytokines.[29] Thus, it is possible that Nef affects the functions of macrophages by differently modulating the activities of M-CSF and GM-CSF, contributing to the uncontrolled immune system. However, little is known of the molecular mechanisms by which Nef differently modulates the activities of these cytokines, through the common target Hck. In this study, we therefore attempted to clarify how the Nef-Hck interaction caused the impaired activation of Fms.

Methods

Hematopoietic cell lines and culture conditions

Human myeloid leukemia TF-1 cells[30] were maintained with RPMI1640 medium supplemented with 10% FCS and 2 ng/mL recombinant human GM-CSF (rhGM-CSF; PeproTech, Rocky Hill, NJ). TF-1-fms cells,[31] which were obtained by introducing the plasmid pCEF-c-fms encoding the human *c-fms* gene into the TF-1 cells, were maintained with RPMI1640–10% FCS in the presence of 100 ng/mL rhM-CSF (a gift from Morinaga Milk Industry, Kanagawa, Japan) and 200 μg/mL G418 (Calbiochem, Darmstadt, Germany). TF-1-fms-Nef-ER cells[26] were obtained by introducing pEBB-Nef-ER-IRES-puro[32] into TF-1-fms cells, and maintained in the presence of rhM-CSF, G418, and 1.5 μg/mL puromycin (Sigma, St Louis, MO). The plasmid encoded the Nef-ER fusion protein composed of Nef (derived from the NL4–3 strain of HIV-1) and the hormone-binding domain of the murine estrogen receptor (ER).[32] In this system, Nef was basally inactive but it was induced to function by the estrogen analog, 4-hydroxytamoxifen (4-HT; Sigma).[32] We also established TF-1 cells expressing the Nef-ER fusion protein (TF-1-Nef-ER) by using the same plasmid. The transfection was performed with Lipofectin reagent (Invitrogen, Carlsbad, CA), according to the manufacturer's recommendations. Transfected cells were selected in media containing rhGM-CSF and puromycin, followed by limiting dilution to isolate stable clones. The expression of Nef-ER in these clones was determined by Western blotting[26] with anti-Nef rabbit antiserum obtained through the National Institutes of Health (NIH) AIDS Research and Reference Reagent Program (Division of AIDS, National Institute of Allergy and Infectious Diseases, NIH, Bethesda, MD).[33] The cell growth was determined by colorimetric assay with MTT reagent (Sigma), and the absorbance of each culture was measured at 595 nm with a microplate reader (Thermo Electron, Vantaa, Finland). The expression of Fms on TF-1-fms-Nef-ER cells and that of GM-CSF receptors on TF-1-Nef-ER cells was analyzed on a FACSCalibur using Cell Quest Software (Becton Dickinson, Mountain View, CA).[26] Anti-Fms rat monoclonal IgG (clone 12-2D6; Zymed, South San Francisco, CA) was labeled with FITC using Fluorescein Labeling Kit-NH_2 (Dojindo, Kumamoto, Japan). FITC-labeled anti–GM-CSF receptor α chain (clone 4H1) and PE-labeled anti–GM-CSF β chain (clone 1C1) were purchased from eBioscience (San Diego, CA).

Macrophages and nucleofection

Human peripheral blood samples were collected from adults donors after informed consent was obtained in accordance with the Declaration of Helsinki and based on a protocol approved by the Institutional Review Board of the Faculty of Medical and Pharmaceutical Sciences, Kumamoto University. Monocytes were enriched from peripheral blood mononuclear cells by adherence to dishes for 1 hour. Macrophages were prepared by culturing the monocytes with RPMI1640 medium supplemented with 15% FCS and 100 ng/mL rhM-CSF for 5 to 7 days. The nucleofection with the Human Macrophage Nucleofector Kit and the Nucleofector II device (Amaxa, Cologne, Germany) was performed according to the manufacturer's recommendations. In brief, 5×10^5 macrophages were nucleofected with 5 μg plasmid and then cultured with Macrophage-SFM medium (Gibco, Grand Island, NY) supplemented with 15% FCS and 10 ng/mL rhGM-CSF for 8 to 12 hours. The nucleofected macrophages were cultured with GM-CSF, because M-CSF caused the down-regulation of Fms (Figure S2B,C). To identify the Nef-expressing macrophages, we used the pRc/CMV-CD8-Nef plasmid[34] encoding Nef (derived from the SF2 strain of HIV-1) fused to the extracellular/transmembrane regions of CD8. As a control, we used the plasmid encoding only those regions of CD8 (pRc/CMV-CD8).[34] The nucleofected macrophages were detached from the culture dishes using the enzyme-free cell dissociation buffer (Gibco), and then subjected to flow cytometric analysis on a FACSCalibur. Labeled antibodies used were PE-labeled anti-Fms (clone 3-4A4; Santa Cruz Biotechnology, Santa Cruz, CA), APC-labeled anti-CD8 (clone DK25; Dako, Glostrup, Denmark), and PE-labeled anti-CD4 (clone S3.5; Caltag, Burlingame, CA).

293 cell lines, transfection, and plasmids

Human embryonic kidney 293 cells (Invitrogen) were maintained with DME medium supplemented with 10% FCS. We also used 293 cells stably expressing Fms, both Fms and Hck, or CD4. 293-Fms cells were established by transfecting pCEF-c-fms[31] followed by the enrichment of Fms^{high} cells with a JSAN cell sorter (Bay bioscience, Kobe, Japan). 293-Fms/Hck cells were established by further transfecting a human Hck expression plasmid into the 293-Fms cells. For this purpose, Hck cDNA[35] cloned in the vector pIRES2-EGFP (Clontech, Mountain View, CA) was subcloned into pIRES-bleo3 (Clontech). An Hck^{high} clone was isolated from the transfected cells by Western blotting. 293-CD4 cells were established by transfecting pEneoMOS-CD4[36] followed by the enrichment of $CD4^{high}$ cells by the sorting. These cells were maintained with media containing 200 μg/mL G418 or 200 μg/mL phleomycin D1 (Invitrogen), or both. Transient transfection experiments with these 293 cell lines were performed essentially as described previously.[26] In brief, cells grown on a 12-well tissue culture plate were transfected with a total of 1.6 μg plasmid using LipofectAMINE2000 reagent (Invitrogen).

The transient expression of Fms was achieved with pCEF-c-fms. The transient expression of Hck was mostly achieved with Hck cDNA cloned in pcDNA3.1 (Invitrogen), except for the flow cytometric analysis in which Hck cDNA cloned in pIRES2-EGFP was used (Figure 2A). Based on an earlier report,[14] we also prepared constitutive-active (YF and AxxA) and kinase-dead (KE) forms of Hck by using QuikChange II Site-Directed Mutagenesis Kits (Stratagene, La Jolla, CA). The transient expression of Nef was achieved mostly with pRc/CMV-CD8-Nef,[34] the Nef of which was

derived from the SF2 strain of HIV-1. In a selected experiment (Figure 4A), we used Nef of the NL4-3 strain, as the mutants used in the analysis were derived from the strain. WL/AA, LL/AA, and AxxA mutants were provided by A. Adachi (University of Tokushima, Tokushima, Japan) and subcloned into the vector pRc/CMV-CD8. The M20A mutant[37] was also subcloned into this vector.

Western blotting, flow cytometry, and immunofluorescence with 293 cells

The preparation of total cell lysate and Western blotting were performed essentially as described.[26,38] In a selected experiment (Figure 2C), a monolayer of transfected 293 cells was treated with trypsin or control PBS buffer for 3 minutes at room temperature immediately prior to the lysis. Total cell lysate was also subjected to a lectin pull-down assay,[39] using wheat germ agglutinin (WGA)–agarose and concanavalin A (Con A)–agarose (both from Wako, Osaka, Japan). Alternatively, total cell lysate was treated with either endo-β-*N*-acetylglucosaminidase H (Endo-H) or peptide-*N*-glycosidase F (PNGase F) (both from Roche, Mannheim, Germany), according to the manufacturer's recommendations. Primary antibodies used were as follows: anti–N-terminal portion of Fms (H-300; Santa Cruz Biotechnology), anti–C-terminal portion of Fms (C-20; Santa Cruz Biotechnology), anti-Nef rabbit antiserum,[33] anti-Hck (clone 18; Transduction Laboratories, Lexington, KY), and anti-ERK (K-23; Santa Cruz Biotechnology).

The transfected cells were detached from the culture dishes and subjected to a flow cytometric analysis with anti–Fms-PE, anti–CD4-PE, or anti–CD8-APC as above. For immunostaining, cells were directly fixed in 2% paraformaldehyde, permeabilized with ethanol, and stained with primary antibodies for 12 hours followed by labeled secondary antibodies.[40,41] The primary antibodies used were as follows: anti-Fms rat IgG (clone 3-4A4-E4; Abcam, Cambridge, MA), anti-GM130 mouse IgG (Transduction Laboratories), anti-CD8 rabbit IgG (II-160; Santa Cruz Biotechnology), and rabbit IgG specific for Hck phosphorylated at Tyr411 (Santa Cruz Biotechnology). The labeled secondary antibodies used were as follows: anti–rat IgG-AlexaFluo488, anti–mouse IgG-AlexaFluo568, and anti–rabbit IgG-AlexaFluo488 (Molecular Probes, Eugene, OR). Nuclei were stained with DAPI (Molecular Probes). The fluorescent signals were visualized with a BZ-8000 fluorescence microscope (Keyence, Osaka, Japan) equipped with Plan-Fluor ELWD 20×/0.45 objective lenses (Nikon, Tokyo, Japan). Image processing was performed using BZ-Analyzer (Keyence) and Adobe Photoshop software (Adobe Systems, San Jose, CA).

Results

Nef selectively inhibits M-CSF–dependent growth and down-regulates Fms

In this study, we initially attempted to confirm the stimulatory effect of Nef on GM-CSF reported by another group,[25] using the same system in which we found the inhibitory effect on M-CSF.[26] We previously established human myeloid TF-1-fms cells expressing a conditionally active Nef-ER fusion protein.[26,32] Although TF-1-fms was an M-CSF–dependent clone derived from GM-CSF–dependent TF-1 cells,[30,31] TF-1-fms cells lost their growth response to GM-CSF due to long-term maintenance with M-CSF.[42] Thus, we also established TF-1 clones expressing the Nef-ER fusion proteins, the level of which was comparable with that in the pre-established TF-1-fms-Nef-ER clone (Figure S1A, available on the *Blood* website; see the Supplemental Materials link at the top of the online article). The inducible activation of Nef by the estrogen analog 4-HT was verified by the down-regulation of CD4 expression (data not shown). As shown (Figure S1A,B) and consistent with the results of the other group,[25] the activation of Nef did not inhibit but enhanced the GM-CSF–dependent growth of TF-1-Nef-ER cells, albeit slightly. However, the activation of Nef markedly inhibited the M-CSF–dependent growth of TF-1-fms-Nef-ER cells (Figure S1A,C). These results confirmed that Nef did not actively induce the death of these cells but selectively inhibited the activity of M-CSF.

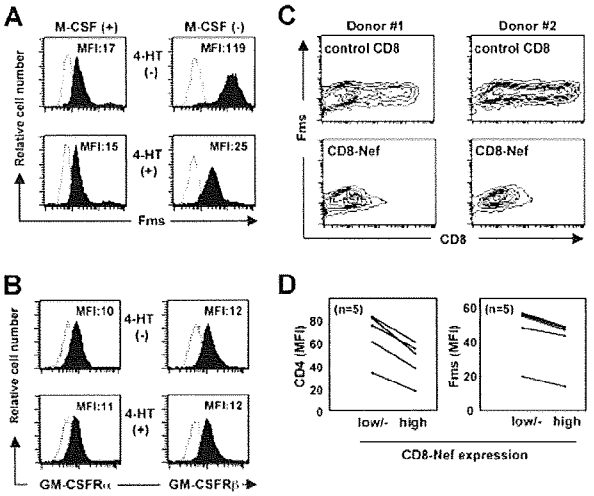

Figure 1. Nef inhibits surface expression of Fms. (A) In the left histograms, TF-1-fms-Nef-ER cells were precultured with M-CSF–containing media in the absence (upper) or presence (lower) of 0.1 mM 4-HT for 24 hours. In the right histograms, TF-1-fms-Nef-ER cells were precultured with M-CSF–free media in the absence (top) or presence (bottom) of 0.1 μM 4-HT for 12 hours. The expression of Fms on these cells was analyzed by flow cytometry with PE-labeled anti-Fms antibody. The mean fluorescence intensity (MFI) of Fms expression is indicated. (B) TF-1-Nef ER cells were precultured with GM-CSF–free media in the absence (top) or presence (bottom) of 0.1 μM 4-HT for 12 hours. The surface expression of GM-CSF receptors was analyzed with FITC-labeled anti-α chain (left) and PE-labeled anti-β chain (right) antibodies. The MFI of GM-CSF receptor expression is indicated. (C) Macrophages were nucleofected with the control CD8 plasmid or CD8-Nef plasmid and then costained with APC-labeled anti-CD8 and PE-labeled anti-Fms. Results with macrophages obtained from 2 different donors are shown as contour plots. (D) As in panel C, the nucleofected macrophages were costained with APC-labeled anti-CD8 and PE-labeled anti-Fms, or with APC-labeled anti-CD8 and PE-labeled anti-CD4. The MFI of the expression of Fms or CD4 in the populations of $CD8^{low/-}$, $CD8^{high}$, $CD8\text{-}Nef^{low/-}$, or $CD8\text{-}Nef^{high}$ was analyzed. The results with macrophages obtained from 5 different donors are summarized.

Next, we carefully examined whether Nef down-regulated the surface expression of Fms, as a possible mechanism for the selective inhibitory effect of Nef on the activity of M-CSF. In a previous study in which TF-1-fms-Nef-ER cells cultured under M-CSF–containing conditions were used, we failed to observe an obvious down-regulation of Fms expression by Nef.[26] However, the effect of Nef might have been underestimated under such conditions, because M-CSF itself down-regulated the expression by inducing the internalization/degradation of Fms.[43] Indeed, the addition of M-CSF caused the down-regulation of Fms in both TF-1-fms-Nef-ER cells (Figure S2A) and primary macrophages (Figure S2B) in a dose-dependent manner and an obvious effect of Nef on the surface level of Fms was not detected under such conditions (Figure 1A left panels). However, under the M-CSF–free Fms-high conditions, a significant reduction in the surface expression of Fms was observed in the Nef-active TF-1-fms-Nef-ER cells (Figure 1A right panels). The surface expression of CD29 (integrin β1), CD33, and CD54 (ICAM-1) was unaffected by the same treatment (data not shown). Furthermore, such down-regulation was not observed with the α chain and β chain of GM-CSF receptors (Figure 1B). Thus, the inhibitory effect of Nef on the activity of M-CSF but not of GM-CSF was likely to be due to the selective down-regulation of Fms expression.